People's Democratic Republic of Algeria
Ministry of Higher Education and Scientific Research
University of Kasdi Merbah Ouargla
Faculty of New Information Technologies and Communication
Department of Electronic and Telecommunications

ACADEMIC MASTER DISSERTATION

Field : Science and Technology

Sector : Electronics

Specialty : Electronics of Embedded systems

Presented by :

ABDI Abdeljawad

BABZIZ Mohammed Yacine

ZEGAOU Youcef

Theme

Direct power control of two-level grid-connected converters using fuzzy logic

Publicly defended on **25/06/2024**, before the jury composed of :

Mr.	BENCHABANE Abderrazak	MCA	UKMO	President
Mr.	RACHEDI Mohamed Yacine	MCA	UKMO	Examiner
Mr.	MEHAOUCHI Azeddine	MAA	UKMO	Supervisor
Mr.	KADRI Farid	MAA	UKMO	Co-Supervisor

DEDICATION

I dedicate all our gratitude and virtues to our dear parents who helped us and spared no effort in educating us through their sacrifices. Let them find here a testimony of our deep respect and infinite appreciation. To Father Youssef and Mother Zainab, I thank you for everything, nothing can describe your greatness to me. To our brothers and sisters, to those who always depend on us, to our mothers, to our aunts and uncles, to our dear cousins, and to our entire family. To all our friends and colleagues in this promotion. To all those who participated directly or indirectly in the accomplishment of this work and who wish us success.

ABDI abdeljawad

DEDICATION

I dedicate this dissertation to my family and friends for their unwavering support and encouragement throughout my academic journey. To my parents, my Father Bahmed and my Mother Lalla, I thank you for everything, nothing can describe your greatness to me. Thank you for your endless love and belief in my potential. To my mentors and professors, for their guidance and inspiration. And to all my friends and colleagues, for their camaraderie and support. This work is a testament to your influence and support.

ZEGAOU Youcef

DEDICATION

This dissertation is dedicated to my family, whose unwavering support and encouragement have been my guiding light throughout this journey. To my parents, my Father Abdelwahab and Mother Saida, I thank you for everything, nothing can describe your greatness to me. for your endless sacrifices and belief in my potential, and to my siblings, for their constant motivation and understanding. To my mentors and professors, for their invaluable guidance and knowledge. Lastly, to my friends and colleagues, for their camaraderie and support. This work is a testament to your faith in me and the collective efforts that have brought this project to fruition. Thank you.

BABZIZ Mohammed Yacin

Remerciement

First of all, we thank God Almighty for giving us courage, patience and strength during all these years of study and thanks to him we were able to accomplish this work.

We would like to express our thanks and gratitude to our supervisor Azeddine Mehaouchi and co-supervisor Farid Kadri for the trust he gave us to guide this work, without stopping to encourage us and push us towards the horizons of scientific research.

Thanks also to the Department of Electronics and Communications at the University and all the professors who taught us over the years. Thanks also to the members of the jury who agreed to judge this work.

Thanks also to the Electrical Engineering Laboratory at the Scientific Research Center at the University of Ouargla.

Finally, we also thank all our families and the people who helped us directly or indirectly, in writing this work.

ملخص

تركز هذه المذكرة على توليف ومحاكاة نظام عاكس ثلاثي الأطوار ذي مستويين متصل بالشبكة. تقارن الدراسة بين استراتيجيتين للتحكم: التحكم المباشر في الطاقة التقليدي (DPC) ونهج التحكم المباشر في الطاقة المعتمد على المنطق الضبابي ($FDPC$) بالذكاء الاصطناعي. تستبدل تقنية $FDPC$ جدول التبديل، ومقارنات التباطؤ، وتحديد القطاع المستخدم في DPC التقليدي بوحدة تحكم منطقية غامضة.
تُوضح نتائج المحاكاة التي أجريت باستخدام $MATLAB/SIMULINK$ فعالية وحدة التحكم الضبابية المقترحة في تنظيم قدرات الخرج النشطة وغير الفعالة بشكل مستقل. يكشف التحليل المقارن لنتائج المحاكاة أن $FDPC$ يتفوق على DPC التقليدي من حيث الاستجابة الديناميكية، والمتانة، وجودة الطاقة بسبب انخفاض التشوه التوافقي الكلي (THD).

الكلمات المفتاحية: الطاقة النشطة والتفاعلية ، التحكم المباشر في الطاقة(DPC) التحكم المباشر في الطاقة القائم على المنطق الضبابي($FDPC$)، عاكس ذو مستويين موصول بالشبكة .

Abstract

This dissertation focuses on the synthesis and simulation of a two-level three-phase grid-connected inverter system. The study compares two control strategies: the conventional direct power control (DPC) and an artificial intelligent fuzzy logic-based DPC approach (FDPC). The FDPC technique replaces the switching table, hysteresis comparators, and sector identification used in classical DPC with a fuzzy logic controller.
Simulation results conducted using MATLAB Simulink demonstrate the proposed fuzzy controller's efficacy in independently regulating active and reactive output powers. Comparative analysis of simulation results reveals that FDPC outperforms conventional DPC in terms of dynamic response, robustness, and power quality due to reduced total harmonic distortion (THD).

Keywords: Active and reactive power, Direct power control (DPC), Fuzzy-based direct power control (FDPC), Two-level grid-connected inverter.

Résumé

Ce mémoire se concentre sur la synthèse et la simulation d'un système d'onduleur triphasé à deux niveaux connecté au réseau. L'étude compare deux stratégies de contrôle : le contrôle direct de puissance (DPC) conventionnel et une approche de DPC d'intelligence artificielle basée sur la logique floue (FDPC). La technique FDPC remplace la table de commutation, les comparateurs à hystérésis et l'identification des secteurs utilisés dans le DPC classique par un contrôleur à logique floue.
Les résultats de simulation réalisés à l'aide de MATLAB Simulink démontrent l'efficacité du contrôleur flou proposé pour réguler indépendamment les puissances active et réactive de sortie. L'analyse comparative des résultats de simulation révèle que le FDPC surpasse le DPC conventionnel en termes de réponse dynamique, de robustesse et de qualité de puissance, grâce à une distorsion harmonique totale (THD) réduite.

Mots Clée : Puissance active et réactive, Contrôle direct de puissance (DPC), Contrôle direct de puissance basé sur la logique floue (FDPC), Convertisseur à deux niveaux connecté au réseau.

Contents

List of Figures

List of Tables

Nomenclature

Acronymes / Abréviations

α, β	Axes of the park reference
Δp	Active power Errors
Δq	Reactive power Errors
a, b, c	Correspond to the three phases
AC	Alternating Current
DC	Direct Current
DPC	Direct Power Control
H_p	keeps him away from the hestericized blonde
H_q	keeps him away from the hestericized blonde
I_a	the current in the arm a
I_b	the current in the arm b
I_c	the current in the arm c
p	active power
P_r	active power reference
PWM	Pulse Width Modulation
q	reactive power
Q_r	Reactive power reference
$S_{a,b,c}$	The inverter arm a, b or c switch (two levels)

ST	Switching Table
T_e	Simpel Time
THD	Deformation coefficient
$V - DPC$	Voltage Vector for Direct Power Control
$V_a,\ V_b,\ V_c$	the three-phase network voltage
V_i	Command vector
V_M	the maximum value
V_{dc}	DC supply voltage of the voltage inverter

General Introduction

Energy is essential for all our activities, it opens the way for innovations New sectors that constitute engines for job creation and inclusive growth Shared prosperity [4]. Yet more than 733 million people on the planet live without it Electricity. One of the main devices of power transformers is the conventional voltage inverter two-level network connected, which is used to convert direct current into Alternating current Recently, various control strategies have been developed to improve its reliability, efficiency, and safety by engineers and researchers. Among these control methods, the strategy of direct control of power emerged as a means of control Suitable for grid connected inverters as it allows efficient and direct control active and reactive forces, moreover, do not require any modulation block or loops current regulation [4]. On the other hand, control of dual-level converters is crucial interesting. DPC has been applied to various grid-connected converter applications such as renewable energy sources interface, active power filters, and DC-AC converters. Extensive research has been done on improving the DPC strategy in terms of reducing torque/power ripple, improving steady-state performance, and extending it to multilevel inverters [5]. The main advantages of DPC are its simple structure, fast dynamic response, and decoupled control of active and reactive power [6].
Voltage inverters constitute an essential function of the electronics of power. They are present in the most varied fields of application. The strong evolution of this function was based, on the one hand, on the development of semi– fully controllable, powerful, robust and fast drivers and on the other hand, on the almost generalized use of so-called Pulse Width Modulation techniques (MLI), as well as the progress made in the field of microcomputing. Despite their advantages, conventional (two-level) inverters are limited to the applications of low and medium power and low voltage only (1.4kV, 1 MVA) [7]. On the other hand, the control of two-level and multi-level inverters is a topic very interesting. direct power control (DPC) is become an excellent control technique. The main idea of the proposed DPC initially by Ohnishi (1991) and then developed by Noguchi and Takahashi in 1998 [7].

The goal of direct power control was to eliminate the block of display adjustment Pulse (MLI) and internal regulation loops of controlled variables, by Replacement with a predefined switching table, whose inputs are trace errors The reference for active, reactive and output power is the control vector . The different configurations of DPC, identified in the literature, are divided into two parts Categories: DPC using voltage vector (V-DPC) and DPC using virtual flow witch the detailed configurations are Based on virtual flow calculation. in [8], the authors propose linking principle of DPC with vector pulse width modulation (SVM). To obtain a fixed switching frequency without using a table Switch [9].

The objective of this work is to conduct a comprehensive modeling and simulation study of a two-level grid-connected inverter system. The primary aim is to evaluate the system's in effectiveness in efficiently compensating for both active and reactive power drawn from the grid, while ensuring a robust dynamic and transient response. By proposing an adequate solution to compensate for active and reactive power compensation in electrical networks, this research endeavors to contribute to the field of power quality enhancement and grid stability improvement. To achieve this, a three-phase two-level inverter controlled by direct power control (DPC) methods is employed. Specifically, the classic DPC and an artificially intelligent fuzzy logic-based DPC approach are investigated and comparatively analyzed in terms of their respective performances for active and reactive power compensation.

This dissertation is divided into three chapters.
- The first chapter focuses on the modeling and control of a two-level inverter connected to the grid. It involves modeling the various components, including the two-level inverter, the connection filter, and the electrical network. The inverter is controlled by the conventional DPC technique, which regulates the active and reactive power.
- The second chapter introduces an alternative control technique based on fuzzy logic. This approach replaces the switching table and hysteresis controllers used in classical DPC with a fuzzy logic controller, offering a different control strategy.
- In the third chapter, a comparative analysis between the conventional DPC and the proposed fuzzy DPC methods is conducted. Through matlab/simulink simulations of the two-level grid-connected inverter, this analysis evaluates the performance and efficacy of the two control strategies.
- Finally, the dissertation concludes with a general summary and concluding remarks.

Chapter 1

Direct power control for grid-connected two-level inverter

1.1 Introduction

Direct Power Control DPC is a control strategy for grid-connected voltage source inverters that directly controls the active and reactive power without using a modulator or coordinate transformation. The DPC is an attractive control strategy for grid-connected inverters due to its simple implementation and excellent dynamic performance in controlling active and reactive power. This system incorporates an inverter that directly injects power into the grid, controlled by the DPC strategy. The DPC operation relies on the Switching table, sector, active and reactive power errors. Ultimately, DPC facilitates direct control over the power injected into the grid.

This chapter presents a study of a two-level inverter connected to the electrical grid, controlled by DPC based on a switching table. We present the modeling of the three-phase two-level inverter, the RL connection filter, and the electric grid. Subsequently, we study the DPC control, including the active and reactive powers, vector representation, hysteresis controller, sector identification, and the switching table. At the end, we present the simulation results of the two-level grid-connected inverter controlled by the DPC control.

1.2 Modeling of the two-level grid-connected inverter

Modeling of a two-level grid-connected inverter involves mathematically representing its electrical behavior, enabling analysis, simulation, and optimization under various operating conditions, such as grid frequency and voltage variation [10]. The modeling process

encompasses the mathematical representation of the inverter's electrical components, including input and output filters, the switching devices (e.g., insulated gate bipolar transistors, or IGBTs), and the DC-link capacitor. Additionally, the model includes the control system responsible for regulating the inverter's output voltage and current to ensure adherence to the desired specifications [10].

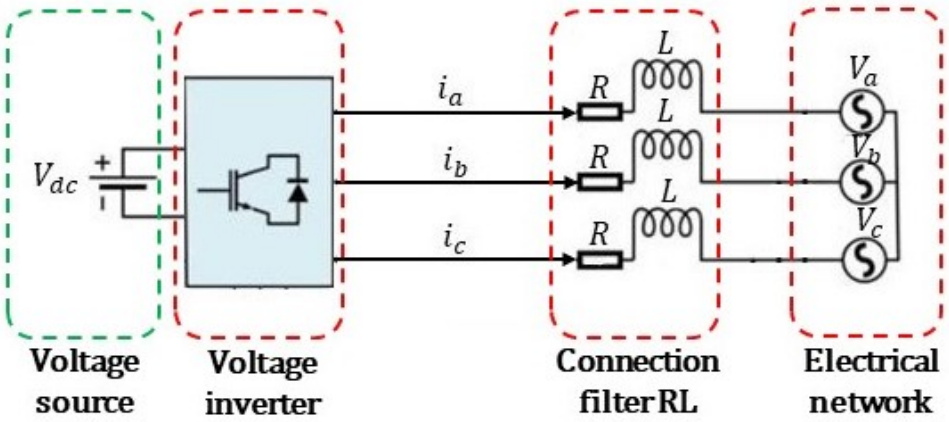

Figure 1.1: The structure of the two-level grid connected inverter.

1.2.1 Three-phase two-level inverter

A three-phase two-level inverter is a type of power converter that converts a fixed DC voltage into a three-phase AC voltage with variable magnitude and frequency [11]. It is called a "two-level" inverter because the output voltage waveform has only two voltage levels: positive and negative. The main components of a three-phase two-level inverter are: Six switching devices (IGBTs or MOSFETs) and a DC voltage source [12].

The inverter operates by switching the six devices in a specific sequence to synthesize the desired three-phase AC output voltage from the DC input [11].

The switches established by the switches, which are supposed to be ideal, are described by a login function. The latter describes their open or closed states. Each switch is associated with a connection function S_X
As :

$$\begin{cases} S_X = 1 \text{ (close)} \\ S_X = 0 \text{ (open)} \end{cases} \tag{1.1}$$

With $_X$= a ,b ,c : Number of the switch of the arm $_X$

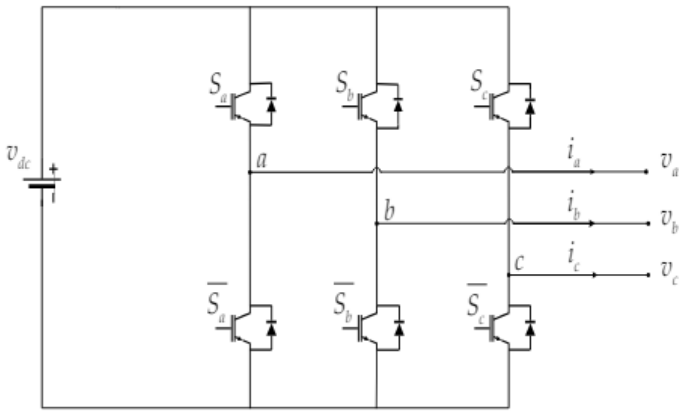

Figure 1.2: Three-phase two-level inverter.

1.2.2 Connection filter RL

The three-phase equivalent circuit of the RL filter (Fig. 1.3) With reference to this figure, R denotes the filter resistance, L the filter inductance, and L the parasitic inductance of the resistor plus the stray inductance in the resistor-to-inductor interface. The resistor parasitic inductance can range from a few H to several tens of mH, depending on the resistor technology (wire wound resistor, anti-inductive resistance, etc). There are two reasons why the filter lowers the load overvoltage [13].

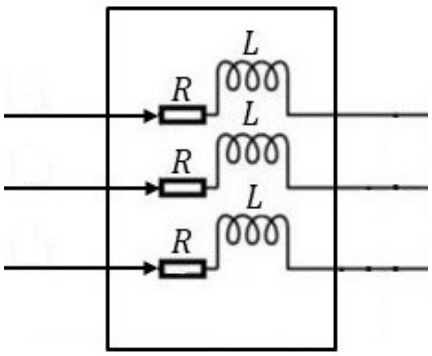

Figure 1.3: The structure of filter RL

1.2.3 Electric network

Figure 1.4 represents the three-phase power grid designed by a three-phase sinusoidal balanced system. As a result :

$$\begin{cases} V_a = V_m sin(t) \\ V_b = V_m sin(t - \frac{2\pi}{3}) \\ V_c = V_m sin(t - \frac{3\pi}{4}) \end{cases} \tag{1.2}$$

With V_m is the maximum value of the sinusoidal voltage and $= 2\pi f$ is the pulsation.

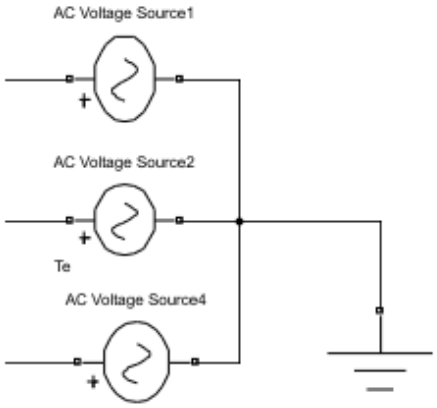

Figure 1.4: The structure of Network electrical

1.3 Direct power control for two-level inverter

Figure 1.5 shows the overall configuration of the direct power control for a two-level inverter connected to the grid. The DPC method operates without a voltage sensor by selecting an appropriate voltage vector from a switching table. This switching table is based on the digitized errors (Sp, Sq) of the instantaneous active and reactive power, obtained from two-level hysteresis regulators, as well as on the angular position of the grid voltage vector. Depending on the angular position, the - plan is divided into twelve sectors, with each sector associated with a specific logical state of the inverter switches. By determining the sector from the grid voltage position and the active/reactive power errors, the DPC scheme selects the appropriate inverter state from the switching table to control the active and reactive power flow [4].

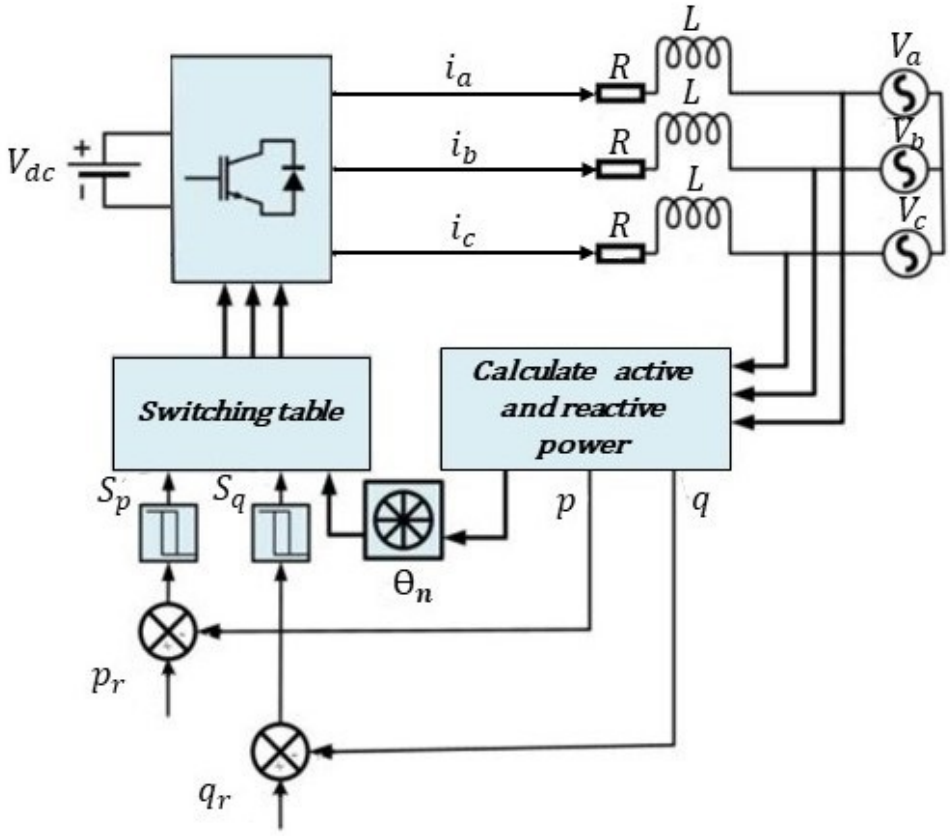

Figure 1.5: Schematic diagram of the two-level inverter DPC control

1.3.1 Active and reactive powers calculation

After transforming the three-phase system into a two-phase system by the Concordia transformation, we can represent the vector V in a space at two dimensions (α,β) by:

$$V = V_\alpha + jV_\beta \tag{1.3}$$

Where Vα and Vβ are the projections of the vector V in the fixed system (α,β) given by:

$$\begin{bmatrix} V_\alpha \\ V_\beta \end{bmatrix} = \sqrt{\frac{2}{3}} \begin{bmatrix} 1 & -\frac{1}{2} & -\frac{1}{2} \\ 0 & \frac{\sqrt{3}}{2} & -\frac{\sqrt{3}}{2} \end{bmatrix} \begin{bmatrix} V_a \\ V_b \\ V_c \end{bmatrix} \tag{1.4}$$

The Iα and Iβ are the projections of the vector I in the fixed system (α,β) given by:

$$\begin{bmatrix} I_\alpha \\ I_\beta \end{bmatrix} = \sqrt{\frac{2}{3}} \begin{bmatrix} 1 & -\frac{1}{2} & -\frac{1}{2} \\ 0 & \frac{\sqrt{3}}{2} & -\frac{\sqrt{3}}{2} \end{bmatrix} \begin{bmatrix} I_a \\ I_b \\ I_c \end{bmatrix} \tag{1.5}$$

The active power p and the reactive power q can be calculated as :

$$\begin{bmatrix} p \\ q \end{bmatrix} = \begin{bmatrix} V_\alpha & V_\beta \\ -V_\beta & V_\alpha \end{bmatrix} \begin{bmatrix} I_\alpha \\ I_\beta \end{bmatrix} \tag{1.6}$$

1.3.2 Vector representation

Figure (1.6) illustrates the vector representation in the complex plane of the six active voltage vectors that can be generated by the inverter. As observed, the switching combinations (111) and (000) result in zero vectors. These active vectors form the switching hexagon or the vector diagram of the two-level inverter [10]. The switching hexagon provides a convenient graphical representation of the available voltage vectors, facilitating the selection of appropriate vectors for DPC based on the instantaneous active and reactive power flow. In the vector diagram, each active vector corresponds to a specific switching state of the inverter's three-phase legs. The amplitude and angle of these vectors determine the instantaneous voltage applied to the grid, directly influencing the active and reactive power exchange.

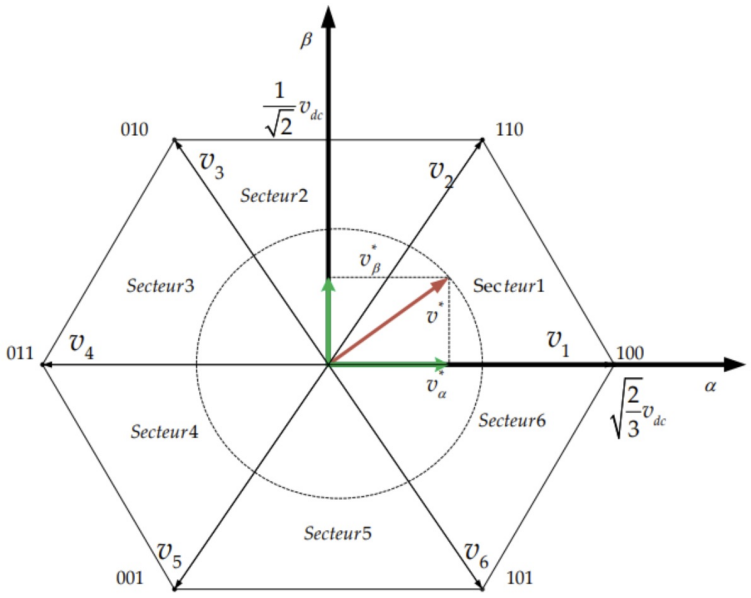

Figure 1.6: Vector diagram of two-level inverter

Knowing that the closure where the simultaneous opening of the two switches of the same arms leads to the risk of destruction of semiconductor components either by overcurrent current either by over voltage, it is essential to carry out an additional order between the Two S_X and $\overline{S}_X$ switches, This leads to the following logical relationship [14].

$S_X = \overline{S}_X$

Where Vα and Vβ can be expressed as a function of the connection functions by the following relation:

$$\begin{bmatrix} V_\alpha \\ V_\beta \end{bmatrix} = \sqrt{\frac{2}{3}} V_dc \begin{bmatrix} 1 & -\frac{1}{2} & -\frac{1}{2} \\ 0 & \frac{\sqrt{3}}{2} & -\frac{\sqrt{3}}{2} \end{bmatrix} \begin{bmatrix} S_a \\ S_b \\ S_c \end{bmatrix} \tag{1.7}$$

Table (1.1) represents the different states of the two-level inverter and the coordinates of the output voltage vector vi in the plane corresponding to each state.

Table 1.1: States of the two-level inverter and the coordinates of the vector vi in the α β plane

S_a	S_b	S_c	V_α	V_β	V_i
0	0	0	0	0	v_0
1	0	0	$\sqrt{\frac{2}{3}}V_dc$	0	v_1
1	1	0	$\sqrt{\frac{1}{6}}V_dc$	$\sqrt{\frac{1}{2}}V_dc$	v_2
0	1	0	$-\sqrt{\frac{1}{6}}v_dc$	$\sqrt{\frac{1}{2}}V_dc$	v_3
0	1	1	$-\sqrt{\frac{2}{3}}V_dc$	0	v_4
0	0	1	$-\sqrt{\frac{1}{6}}V_dc$	$-\sqrt{\frac{1}{2}}V_dc$	v_5
1	0	1	$\sqrt{\frac{1}{6}}V_dc$	$-\sqrt{\frac{1}{2}}V_dc$	v_6
1	1	1	0	0	v_7

1.3.3 Hysteresis controller

Power control using hysteresis consists of maintaining the power in a band enveloping its reference. Whenever the power violates this band, a switching command is issued to the inverter switches, illustrating the principle of fixed-band, two-level hysteresis power control. The difference between the reference and measured powers is applied as an input to a hysteresis comparator, whose output provides the control signal for the corresponding inverter leg, as shown in Figure (1.7) [10]. The bandwidth of hysteresis regulators

significantly impacts the inverter's performance, particularly in terms of harmonic current distortion and avrege switching frequency. The outputs of the hysteresis regulators given by the boolean variables Sp and Sq, indicate whether the active and reactive power errors exceed the upper or lower hysteresis bands. By employing hysteresis comparators for active and reactive power control, the DPC scheme can effectively regulate the power flow while maintaining it within the desired hysteresis band, ensuring stable and accurate power exchange with the grid.

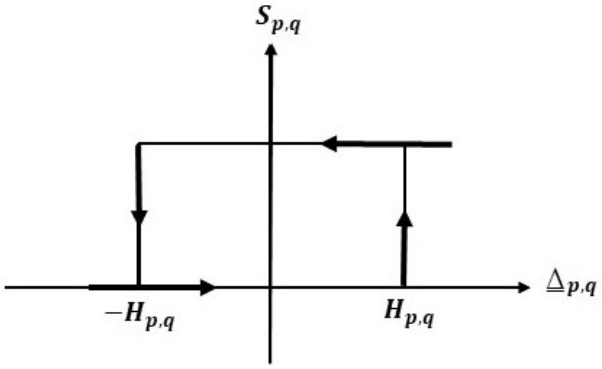

Figure 1.7: Hysteresis comparator operating principle

Operating principle of hysteresis comparator. [2] The outputs of the hysteresis regulators given by the Boolean variables Sp and Sq, indicate the overshoots or undershoots of the power errors according to the logic below:

$$S_p = \begin{cases} 1, P_{ref} - p > h_p \\ 0, P_{ref} - p < -h_p \end{cases} \tag{1.8}$$

$$S_q = \begin{cases} 1, q_{ref} - q > h_q \\ 0, q_{ref} - q < -h_q \end{cases} \tag{1.9}$$

1.3.4 Identification of the sector

The DPC algorithm divides the voltage space vector plane into a number of sectors (typically 6 or 12 sectors), as shown in Figure 1.8. The current sector is determined based on the instantaneous values of the grid voltage. This sector information is used to select the appropriate switching states for the inverter [4].

$$(n-1)\frac{\pi}{6} \leq \theta_n \leq n\frac{\pi}{6}, n = 1, 2...., 12 \tag{1.10}$$

$$(n-1)\frac{\pi}{3} \leq \theta_n \leq n\frac{\pi}{3}, n = 1, 2...., 6 \tag{1.11}$$

The sector number is determined instantly by the given voltage vector position by :

$$\theta = \arctan(\frac{V_\beta}{V_\alpha}) \tag{1.12}$$

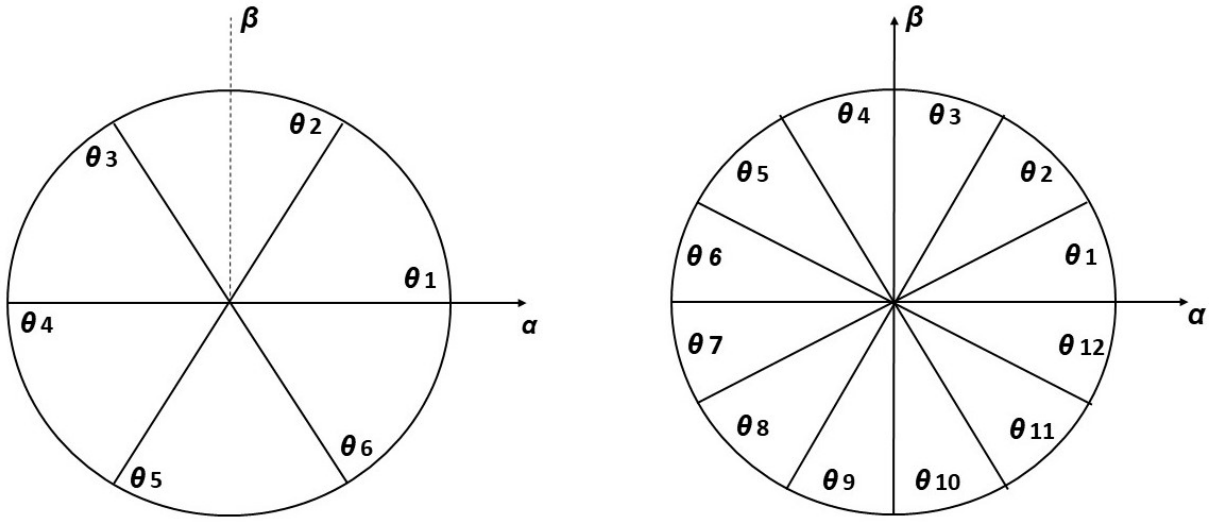

(a) Plane (α, β) divided into 6 sectors **(b)** Plane (α, β) divided into 12 sectors

Figure 1.8: 6 and 12 sectors of the voltage plane used in DPC

1.3.5 Switching table

The DPC uses a predefined switching tables (Tables 1.2, 1.3, 1.4, and 1.5) to select the optimal switching states for the inverter based on the instantaneous errors between the reference and estimated active and reactive power. The switching states are chosen to minimize these power errors [7].These power errors are compared against hysteresis bands using comparators, and the resulting signals, Sp and Sq, are digitized. Additionally, the phase angle of the power source voltage vector is converted to the digitized signal, . The digitized error signals Sp and Sq, along with the digitized voltage phase angle, are inputs to the switching table, which stores every possible switching state (Sa, Sb, Sc) of the inverter. By using the switching table, the optimum switching state of the inverter can be uniquely selected at every specific moment according to the combination of the digitized input signals. The selection of the optimum switching state is performed such that the power errors can be restricted within the hysteresis bands [7]. The switching table plays a crucial role in the DPC control, enabling the intelligent selection of inverter switching states to regulate the active and reactive flow effectively while minimizing the power errors

within the specific hysteresis bounds. several studies proposed a switching table for DPC in two-level inverter for six sectors [1, 2] or twelve sectors [**?**, 3].

Table 1.2: Switching table for 6 sectors proposed by Bouafia et al. [1]

S_p	S_q	S_1	S_2	S_3	S_4	S_5	S_6
0	0	v_6	v_1	v_2	v_3	v_4	v_5
0	1	v_4	v_5	v_6	v_1	v_2	v_3
1	0	v_1	v_2	v_3	v_4	v_5	v_6
1	1	v_2	v_3	v_4	v_5	v_6	v_1

Table 1.3: Switching table for 6 sectors proposed by Eloy-Garcia and Alves. [2]

S_p	S_q	S_1	S_2	S_3	S_4	S_5	S_6
0	0	v_5	v_6	v_1	v_2	v_3	v_4
0	1	v_3	v_4	v_5	v_6	v_1	v_2
1	0	v_1	v_2	v_3	v_4	v_5	v_6
1	1	v_2	v_3	v_4	v_5	v_6	v_1

Table 1.4: Switching table for 12 sectors proposed by Nugoshi et al. [1].

S_p	S_q	S_1	S_2	S_3	S_4	S_5	S_6	S_7	S_8	S_9	S_{10}	S_{11}	S_{12}
0	0	v_7	v_1	v_0	v_2	v_7	v_3	v_0	v_4	v_7	v_5	v_0	v_6
0	1	v_7	v_0	v_0	v_7	v_7	v_0	v_0	v_7	v_7	v_0	v_0	v_7
1	0	v_1	v_1	v_2	v_2	v_3	v_3	v_4	v_4	v_5	v_5	v_6	v_6
1	1	v_2	v_2	v_3	v_3	v_4	v_4	v_5	v_5	v_6	v_6	v_1	v_1

Table 1.5: Switching table for 12 sectors proposed by Baktash et al. [3].

S_p	S_q	S_1	S_2	S_3	S_4	S_5	S_6	S_7	S_8	S_9	S_{10}	S_{11}	S_{12}
0	0	v_6	v_6	v_1	v_1	v_2	v_2	v_3	v_3	v_4	v_4	v_5	v_5
0	1	v_7	v_0	v_0	v_7	v_7	v_0	v_0	v_7	v_7	v_0	v_0	v_7
1	0	v_1	v_1	v_2	v_2	v_3	v_3	v_4	v_4	v_5	v_5	v_6	v_6
1	1	v_2	v_2	v_3	v_3	v_4	v_4	v_5	v_5	v_6	v_6	v_1	v_1

1.4 Simulation of the grid-connected two-level inverter

In this part, we make the simulation study in MATLAB 2021b TOOLBOX simulink of the two-level inverter connected to the network controlled by direct power control DPC. This simulation is made for a electric grid (220V, 50Hz), connection filter (L=0.02H, R=0.1ohm), sources of DC voltage of 600V and sampling time of 10-5 s. For control

method, we take Per equal to 1000W in the first step and at t0=0.2s equal to 3000W and Qre=0 VAR in the first step and at t0=0.3s equal to 1000VAR.

1.4.1 Simulation model

To verify the efficiency of a two-level inverter connected to the grid using the direct power control DPC, the simulation model presented in Figure (1.9) is chosen. This model contains the following elements; DC voltage sources, a three-phase two-level inverter, an RL connection filter, a three-phase current and voltage measuring block, a direct power control, and a three-phase electrical grid.

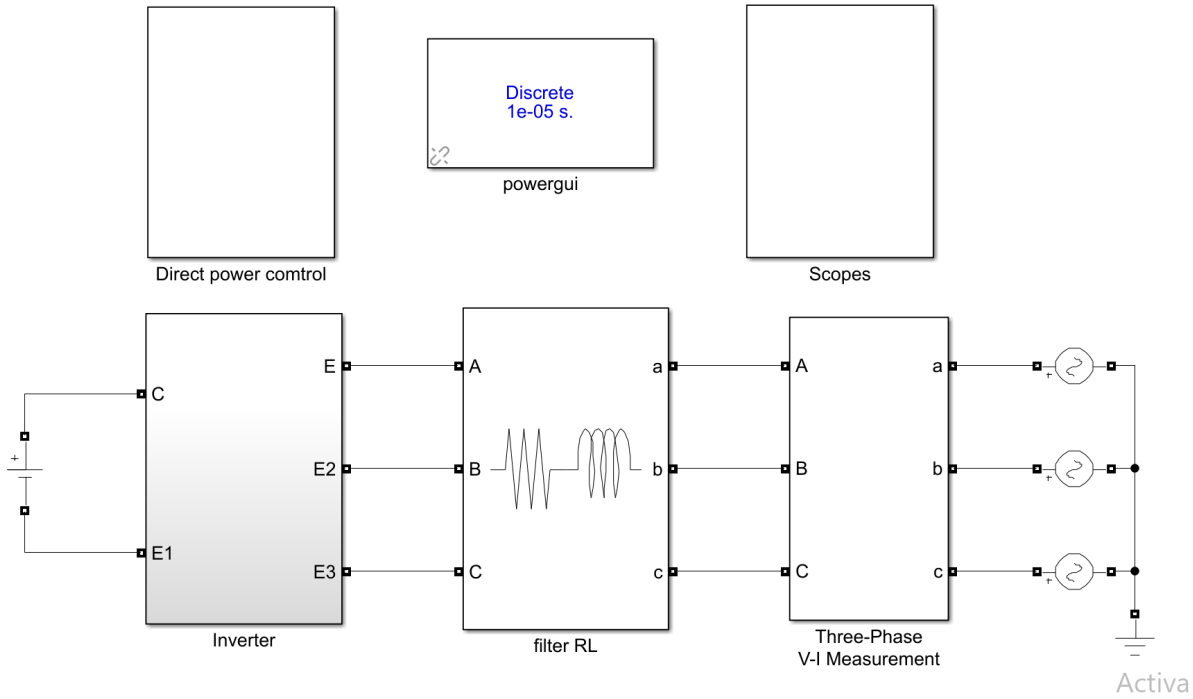

Figure 1.9: Simulink model for grid-connected two-level inverter

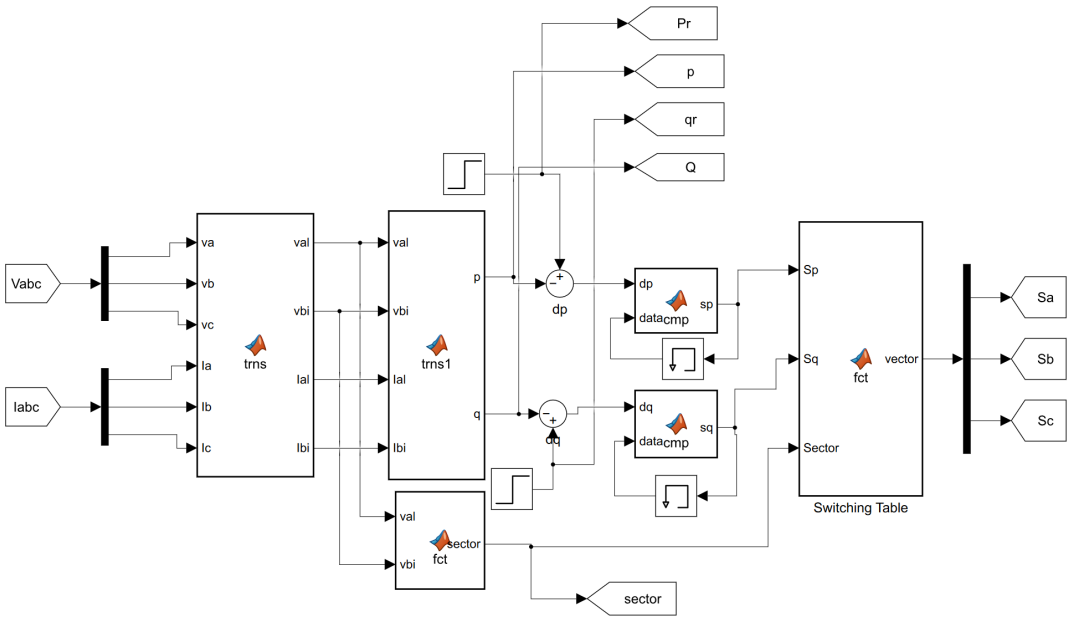

Figure 1.10: Simulink model for Direct Power Control implementation

1.4.2 Results and Interpretation

The figure 1.11 shown the 6-sector, 12-sector, the three-phase voltages in the four switching tables. Figure 1.12, 1.14, 1.16 and 1.18 illustrate the simulation results of the grid-connected two-level inverter for 6 and 12 sector; line currents (Iabc), network voltage Va and line current Ia, reactive power (q), active power (p), reactive power reference (qr), and active power reference (pr). Figure 1.13, 1.15, 1.17 and 1.19 represent the Total Harmonics Distortion THD of the line current Ia.

From these simulation results, it can be observed that the active and reactive powers perfectly follow their reference values in the four switching tables. The values of the current harmonic spectra THD increase with the values of Ts in the four switching tables, and the best switching table according to line current harmonic spectra THD (Figure 1.13) is switching table for 6 sectors proposed by Bouafia et al. [1].

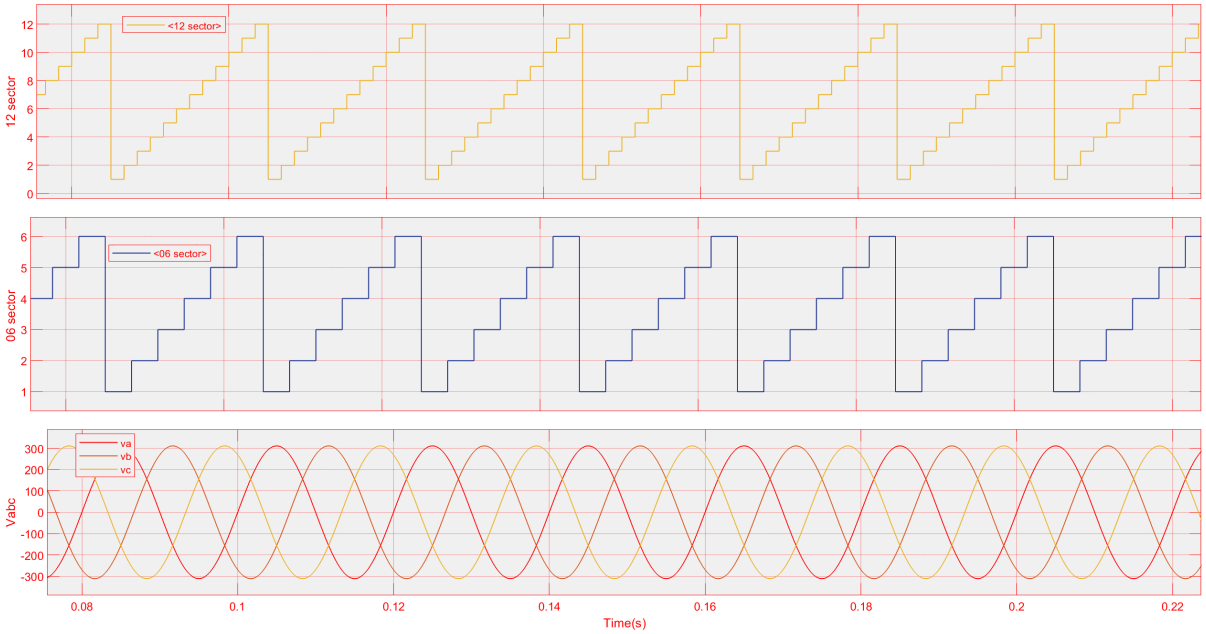

Figure 1.11: Simulation results of the 6-sector, 12-sector, and three-phase grid voltage (Vabc) for DPC for four switching tables.

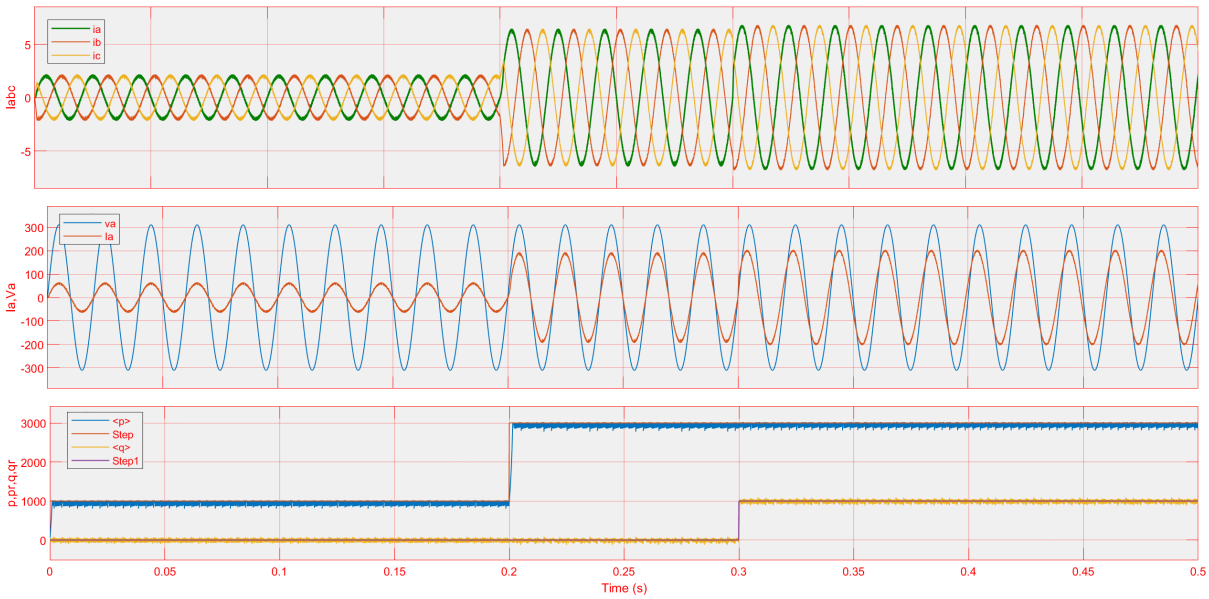

Figure 1.12: Simulation results of the line currents (Iabc, Ia), grid voltage (va), active and reactive powers (pr, p, qr, q) for DPC using switching table proposed by Bouafia et al

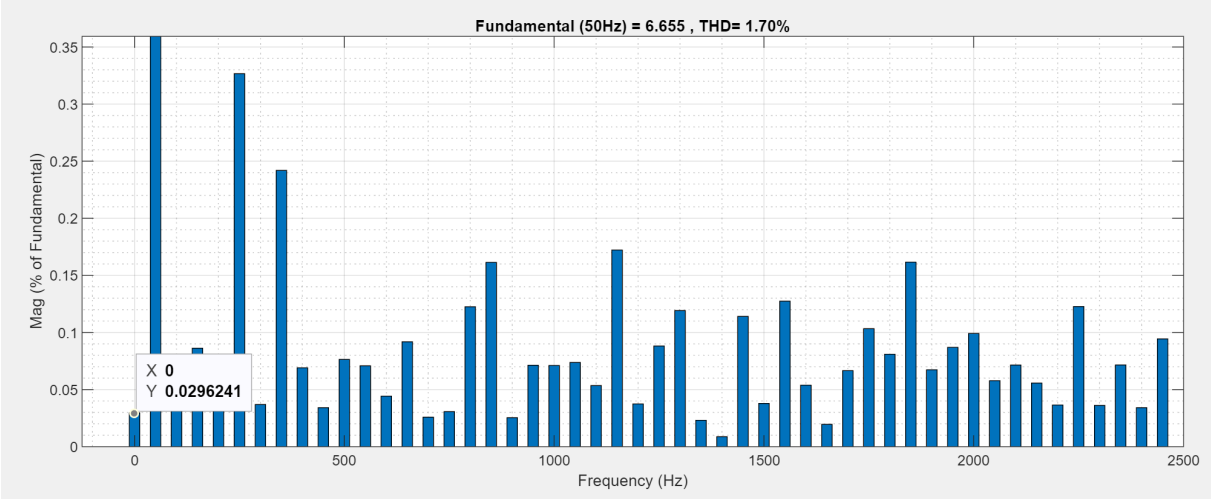

Figure 1.13: THD result of line current for DPC using switching table proposed by Bouafia et al.

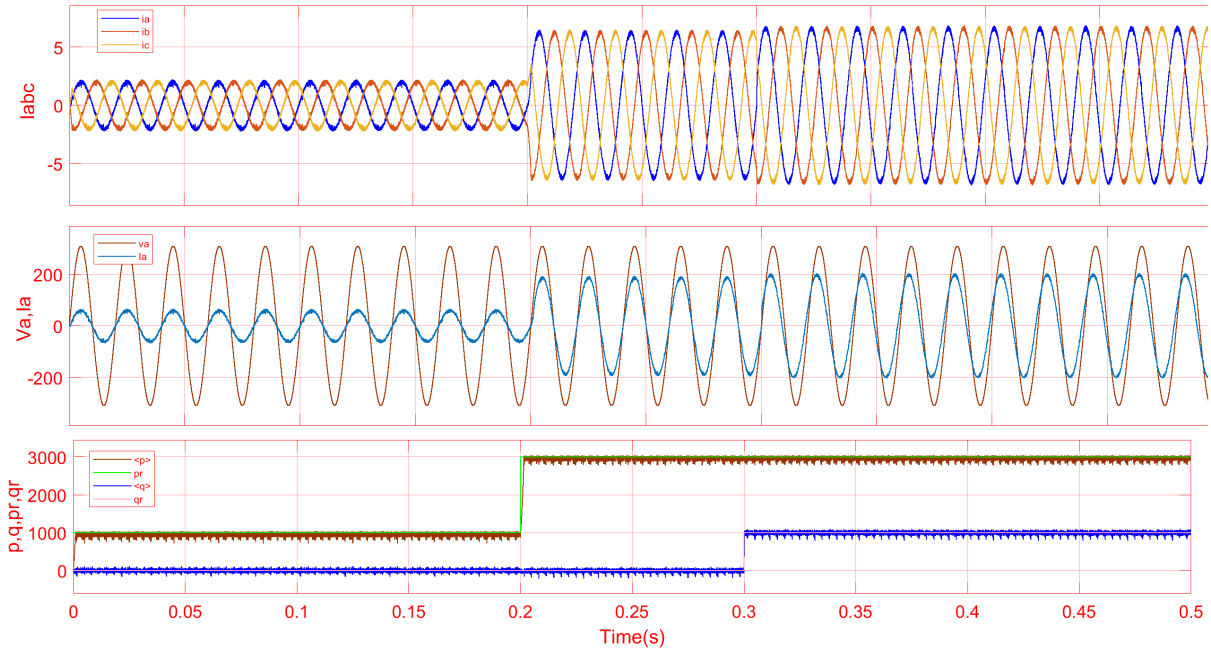

Figure 1.14: Simulation results of the line currents (Iabc, Ia), grid voltage (va), active and reactive powers (pr, p, qr, q) for DPC using switching table proposed by Eloy-Garcia and Alves.

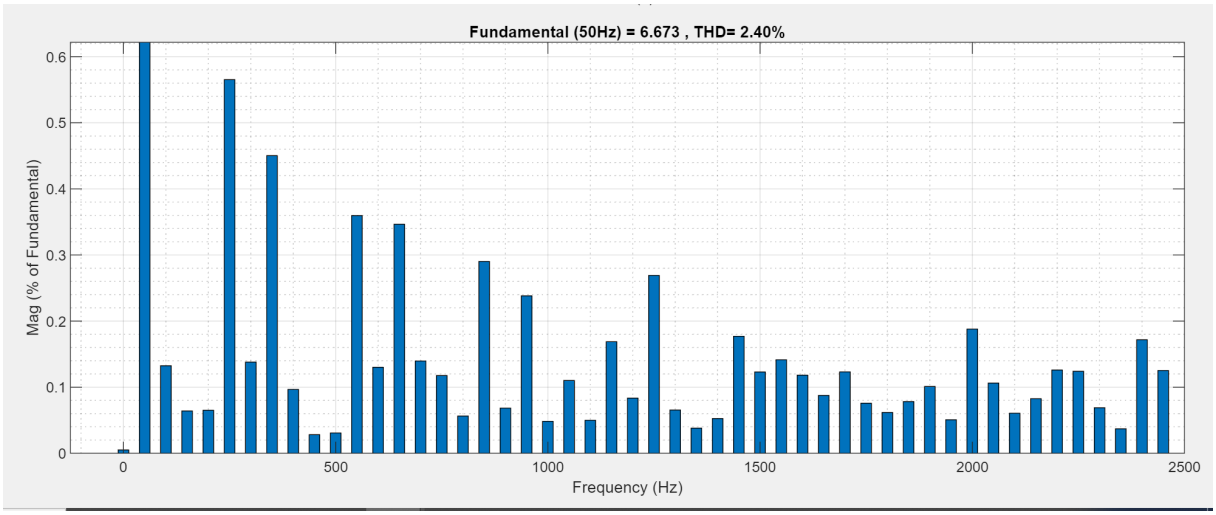

Figure 1.15: THD result of line current for DPC using switching table proposed by Eloy-Garcia and Alves.

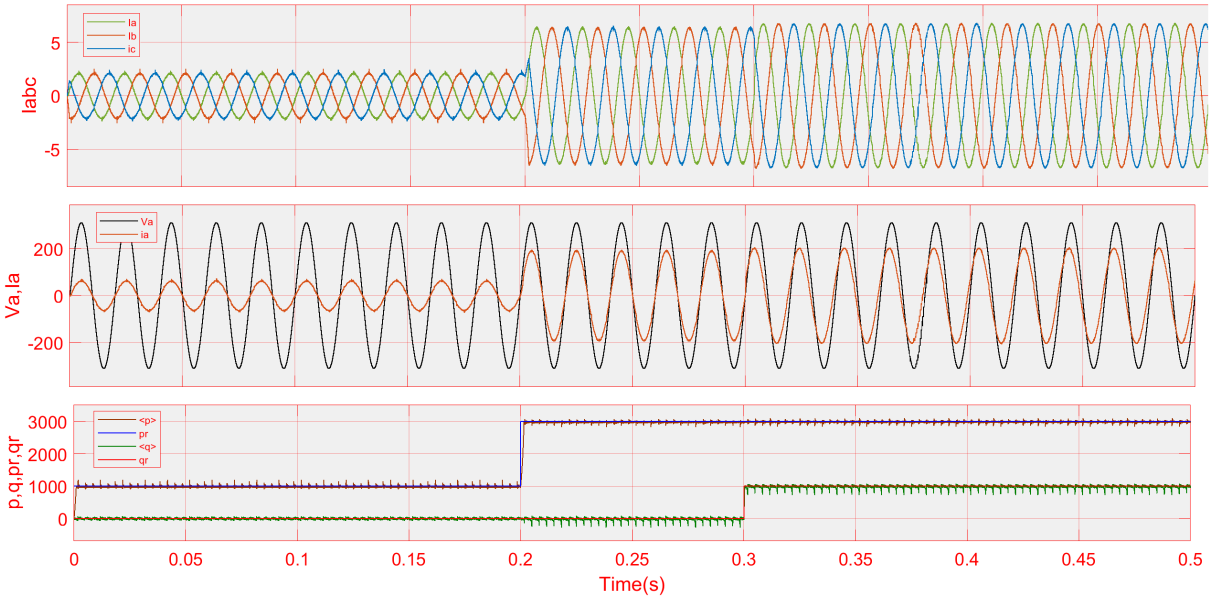

Figure 1.16: Simulation results of the line currents (Iabc, Ia), grid voltage (va), active and reactive powers (pr, p, qr, q) for DPC using switching table proposed by Malinowski et al.

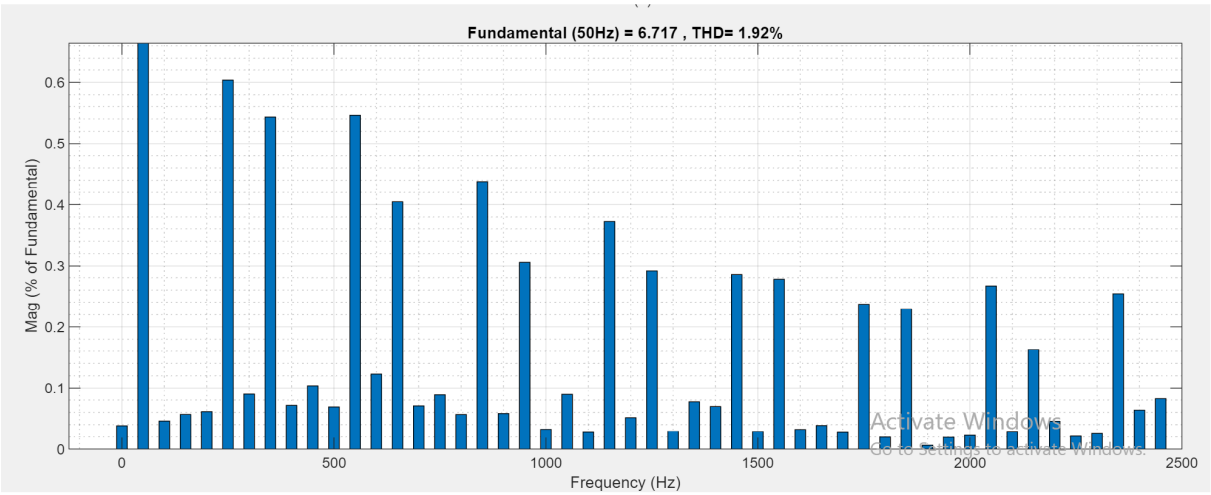

Figure 1.17: THD result of line current for DPC using the switching table proposed by Malinowski et al.

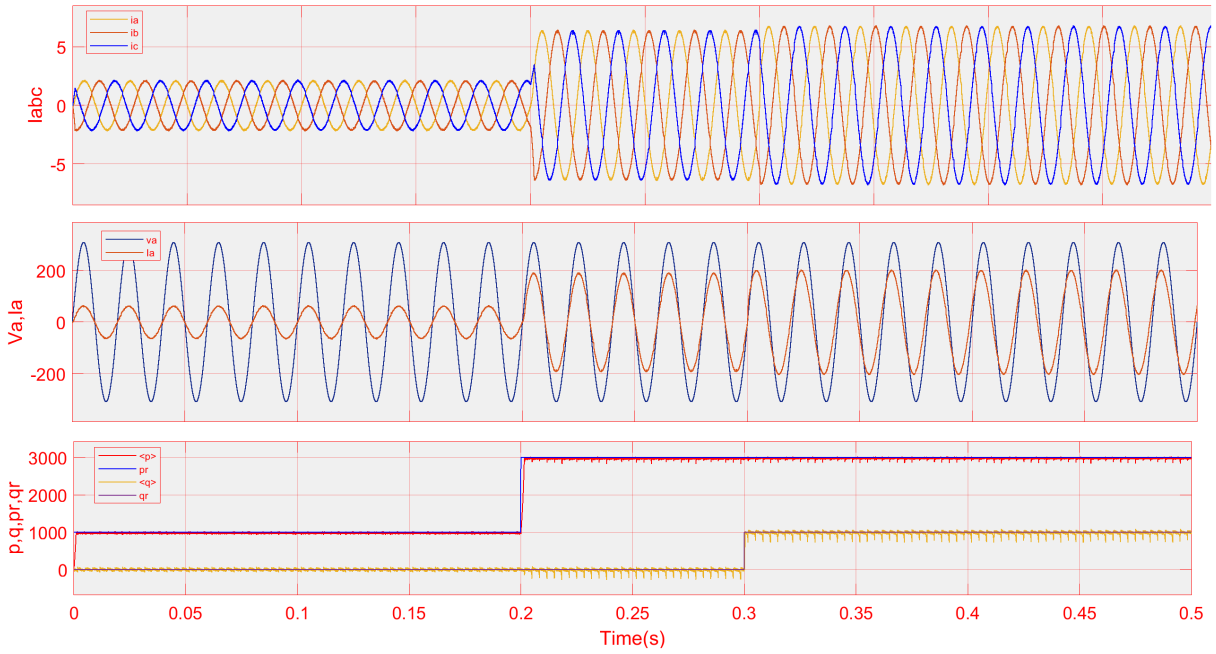

Figure 1.18: Simulation results of the line currents (Iabc, Ia), grid voltage (va), active and reactive powers (pr, p, qr, q) for DPC using switching table proposed by Nugoshi et al.

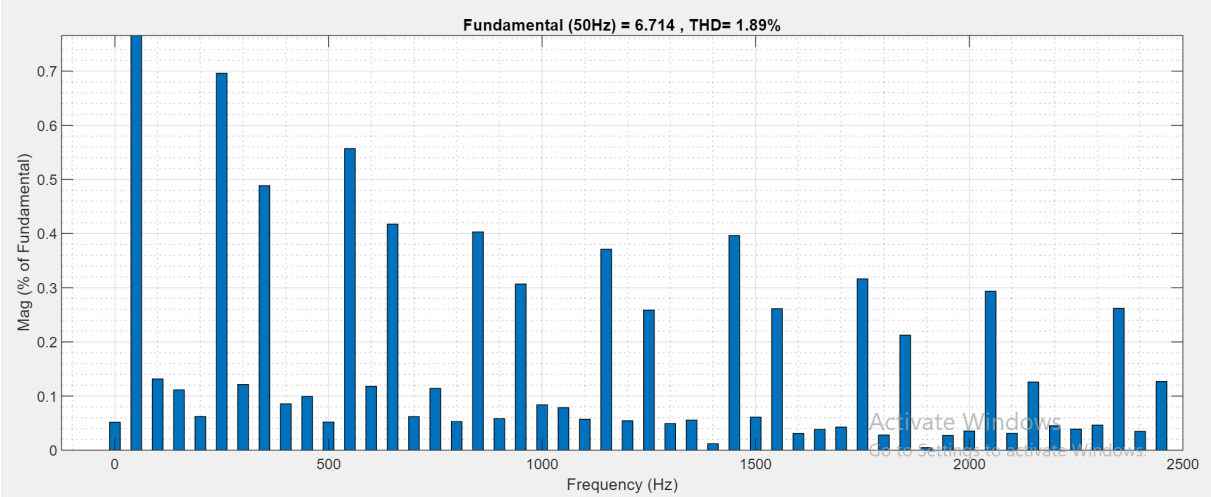

Figure 1.19: THD result of line current for DPC using the switching table proposed by Nugoshi et al.

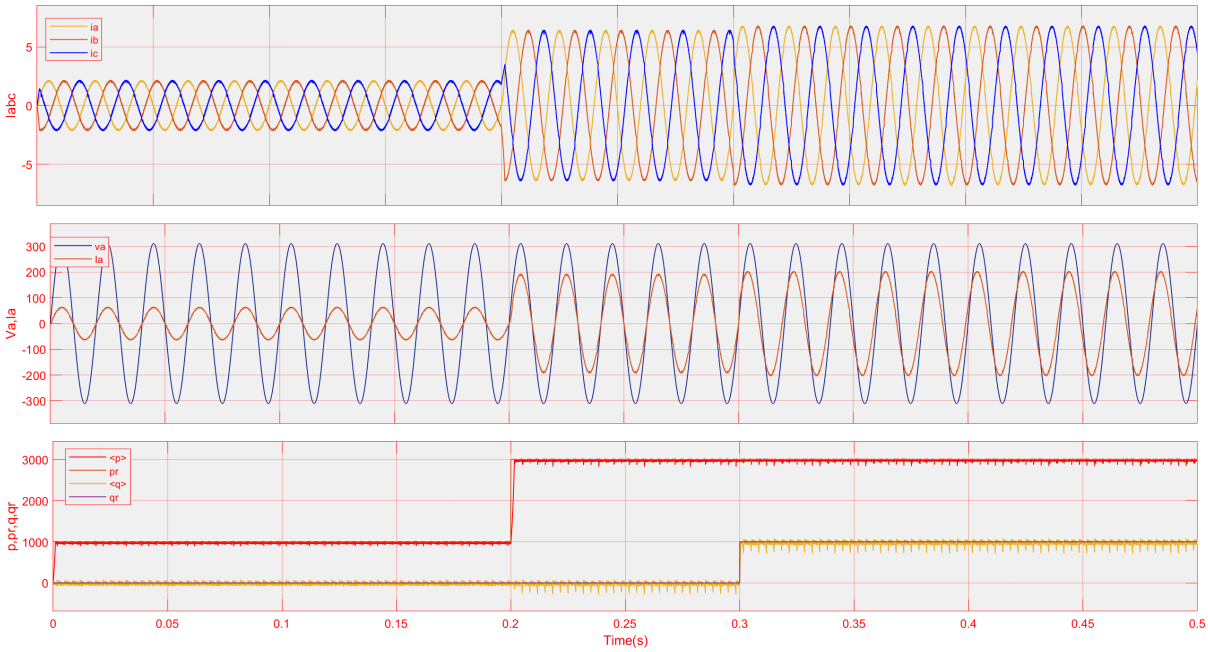

Figure 1.20: Simulation results of the line currents (Iabc, Ia), grid voltage (va), active and reactive powers (pr, p, qr, q) for DPC using switching table proposed by Baktash et al

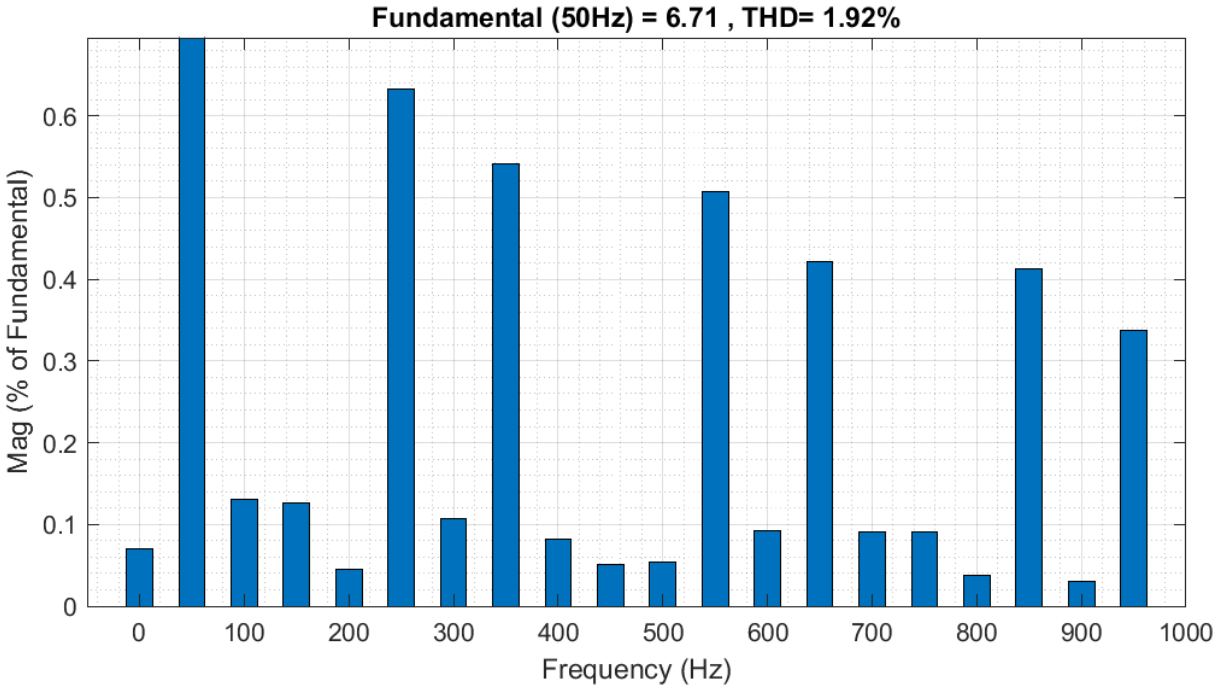

Figure 1.21: THD result of line current for DPC using the switching table proposed by Baktash et al

1.5 Conclusion

In this chapter, we examined the two-level grid-connected inverter system consisting of a constant DC voltage source, a three-phase two-level inverter, an RL filter for grid connection, and an electric grid. After modeling the individual components, we delved into the direct power control strategy in detail. Simulation results were presented, demonstrating the performance of DPC using different switching table configurations.

In the second chapter, we will explore the integration of fuzzy logic with direct power control to achieve enhanced control performance.

Chapter 2

Fuzzy Logic For Direct Power Control

2.1 Introduction

Fuzzy logic is a mathematical description of a process based on the fuzzy set theory. This theory introduced in 1965 by Professor Lotfi Zedah makes it possible to treat proposals or states by several levels of truth [15]. This chapter describes basic concepts, principle and basic elements of fuzzy logic, general structure of a fuzzy system. And finally we present the different elements of a fuzzy controller.

2.1.1 Fuzzy Logic

Fuzzy logic is a technique used in intelligence artificial intelligence allows the formalization of inaccuracies due to a global knowledge of a very complex system and the expression of the behavior of a system by rules. It therefore allows the standardization of the description of a system and the processing of data, both numerical and symbolically expressed by qualifications linguistic. It is based on the mathematical theory of fuzzy sets. This theory, introduced by Zedah, is an extension of classical set theory for the consideration of imprecisely defined sets. It is a formal and mathematical theory in the sense in which Zedah, starting from the concept of membership function to model the definition of a subset of a given universe, developed a complete model of properties and formal definitions. He also showed that this subset theory fuzzy effectively reduces to the theory of classical subsets in the case where the considered membership functions take binary values (0 ,1).

2.1.2 fuzzy logic and classical logic

Classical Boolean logic allows only two states: TRUE or FALSE. The fuzzy logic was proposed by Zadeh in 1965; it allows to express different levels (between 0 and 1), rather

than just 1 or 0. For example: the engine is hot, the engine is very hot. What is the difference between hot and very hot? Or again, a man is high if he measures 170cm. A man is very tall if he is 190cm tall. Where is the dividing line ? Is a man of 180cm tall or very tall? 180.5cm? 179.5cm? Fuzzy logic is a branch of mathematics that allows a computer to model the real world the same way people do. She is concerned about the quantification and reasoning using a language that allows definitions ambiguous, like a lot, little, small, high, dangerous. She takes care of situations where the question that is asked and the answer obtained contain vague concepts [16].
According to fuzzy logic, exact reasoning is a limited case of the reasoning approximate; everything is only a degree. Any logical system can be blurred. The knowledge are interpreted as a collection of elastic or fuzzy constraints of a set of variables. Inference is a process of propagation of constraints elastic bands. Boolean logic is a subset of fuzzy logic.Fuzzy logic makes it possible to accommodate the concept of partial truth: values between completely true and completely false are admitted. We support modes of approximate rather than exact reasoning. Its importance stems from the fact that the human reasoning is approximate [15]

2.2 Fuzzy Logic Operations

Fuzzy logic operations are fundamental in processing fuzzy sets and making decisions based on uncertain or imprecise information. Here are the basic fuzzy logic operations:

1-Fuzzy AND (Intersection):
- Operation: $T[x, y] = min[x, y]$
- Interpretation: The degree of membership of an element in the intersection of two fuzzy sets is the minimum of their individual degrees of membership.

2-Fuzzy OR (Union):
-Operation: $S[x, y] = max[x, y]$
-Interpretation: The degree of membership of an element in the union of two fuzzy sets is the maximum of their individual degrees of membership.

3-Fuzzy NOT (Complement):
-Operation:$C[x] = 1 - x$
-Interpretation: The degree of membership of an element in the complement of a fuzzy set is the complement of its degree of membership in the original set.

4-Fuzzy implication:
- Operation: $T[x, y] = min[x, y]$ (Mamdani implication), $T[x, y] = x * y$ (Product implication), etc.
- Interpretation: Defines the strength of implication between fuzzy propositions. Common implications include Mamdani, Larsen, and Product.

5-Fuzzy aggregation:
- Operation:$S[x_1, x_2, ...x_n]$
- Interpretation: Combining multiple fuzzy values into a single aggregated value, commonly used in fuzzy inference systems.

6-Fuzzy defuzzification:
- Operation: Defuzzification(x)
- Interpretation: Converting fuzzy sets or fuzzy rules into crisp values suitable for decision-making.

These operations form the basis of fuzzy logic systems and are used extensively in various fields, including control systems, artificial intelligence, decision-making, and pattern recognition. [17]

2.3 Fuzzy Control

The proposed fuzzy logic controller includes four basic elements: fuzzyfication unit, base of rules, inference engine and defuzzyfication [15]. The fuzzy regulator is a control system at the base and the internal structure with the main components is shown in page 3.1 as follow:

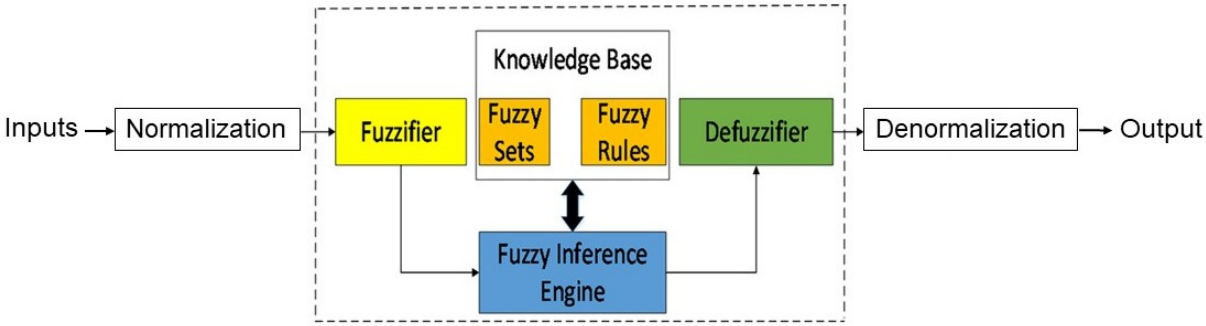

Figure 2.1: Internal structure of a fuzzy controller

2.3.1 Normalization

This first step allows the processing of the input variables of the fuzzy controller. By e.g., calculation of errors (difference between measured quantities and setpoints) and variation errors. Normalized domain use (discourse universe between [-1, 1]) requires a scale transformation, which is carried out through scale factors that transform the physical quantities of the inputs into normalized values belonging to the interval [-1 ,1].

2.3.2 Fuzzification

This is the passage of the domain number and the symbol domain. This place is It is necessary to use the manipulator in the theater of large groups of large groups. Physics are available at certain times or not. She can enter the function at the end membership of a variable to a flow set. It's about the conversion Analog/Digital, as well as the characteristics of the largest and most expensive ones. Transformation into linguistic variables [18].

2.3.3 Base of rules

A fuzzy control rule base consists of a collection of if-then rules that define the behavior of a fuzzy logic controller. These rules use linguistic variables and fuzzy sets to describe the conditions and corresponding actions in the system. The rule base is derived from expert knowledge, heuristic data, or empirical observations and forms the core decision-making framework of the controller [19], To properly understand what a fuzzy rule may mean, it might be useful to start with the meaning of a nonfuzzy rule of the form "if x is A, then y is B", and then to investigate what are the different possible meanings of the rule when A and B becomes fuzzy [20].

2.3.4 Fuzzy inference

Fuzzy inference systems are the core of fuzzy control systems. They map input values to output values using fuzzy rules and membership functions. Fuzzy inference systems are used in various applications, including control systems, image processing, and artificial intelligence, due to their ability to handle imprecise or uncertain information and provide partial truths [21].

2.3.5 Defuzzification

The defuzzification is the operation that used to convert fuzzy variables into crisp values or decisions as one variable number applicable to physical condition:
this is the phase Reverse of Fuzzification , For the method of defuzzification, several strategies of Fuzzification exists, most of them include [22]:
-The mean of maximum method
-The method of averaging maximums
-The center of gravity method
-The weighted average method

Each method has its advantages and is suitable for different application depending on the desired interpretation of the fuzzy logic system's output

2.3.6 Demoralization

This last step transforms the normalized values of the outputs control variables to a values belonging to their respective physical domain

2.4 Application Domain of Fuzzy Logic

2.4.1 Control Systems

which comprises four trol rules provide a convenient way for expressing control policy and domain knowledge. Furthermore, several linguistic variables might be involved in the antecedents and the conclusions of these rules. When this is the case, the system will be referred to as a multi-input-multi-output (MIMO) fuzzy system. For example, in the case of twoinput-single-output (MISO) fuzzy systems, fuzzy control. [23]

2.4.2 Pattern recognition

Fuzzy logic in pattern recognition is a powerful tool for handling the complexities and uncertainties inherent in real-world data. By incorporating fuzzy set theory and fuzzy logic principles, it offers a more comprehensive and flexible approach to pattern recognition, enabling better performance and adaptability in various applications [24].

2.4.3 Consumer electronics

Fuzzy logic has revolutionized consumer electronics by enabling devices to understand and adapt to user preferences, handle ambiguous inputs, and automate tasks more intelligently. This technology has paved the way for smarter, more intuitive, and user-centric consumer electronics [25].

2.4.4 Robotics

Fuzzy logic plays a significant role in robotics, particularly in obstacle avoidance and navigation, fuzzy logic enhances the capabilities of robots by providing a more flexible and adaptive approach to decision-making and control, making them more efficient and effective in various applications [26].

2.4.5 Medicine and health care

Fuzzy logic in medicine and healthcare offers a powerful tool for managing uncertainty and improving decision-making processes. By accommodating the complexities and nuances of human thinking, fuzzy logic can enhance the accuracy and effectiveness of medical diagnoses and treatments, ultimately leading to better patient outcomes [27].

2.5 Development of Fuzzy Controllers for DPC

In order to improve the performance of the conventional DPC, a fuzzy controller has been developed. In this case, the selection of the control vector for each fuzzy rule is based on the sign and the quantity of the variation, unlike the switching table in DPC conventional using the logic outputs of the hysteresis comparators where the selection is based solely on the sign of the variation. For this purpose, the numerical values of the reference tracking errors of the active and reactive powers, ΔP and Δq are converted into fuzzy variables. Two fuzzy sets are used to perform this conversion: N and P

2.5.1 Development of fuzzy controllers to control DPC for 6 sectors

The following diagram represents the part that has been changed, namely the switch table and hysteresis regulators, with fuzzy logic controller

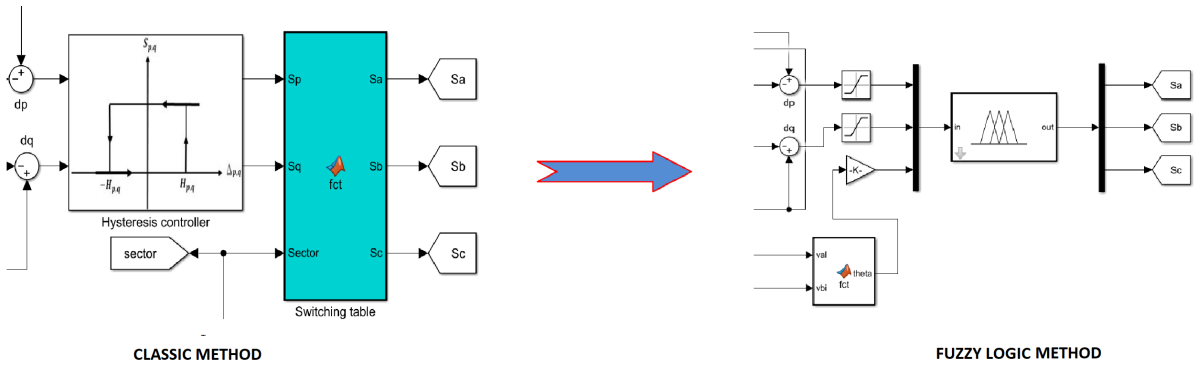

Figure 2.2: Substitutions of switching table and hysteresis regulators by a fuzzy controller

The following figure illustrates the block diagram structure of FDPC (Fuzzy direct power control), where the inputs for the fuzzy controller are the normalized active and reactive power errors (ep and eq) ranging between [-10, 10], and the electrical angle defined between [0°, 360°] degrees

The output corresponds to the voltage vector Vi(Sa, Sb, Sc) of the inverter with the Vi[V1, V2, V3, V4, V5, V6].

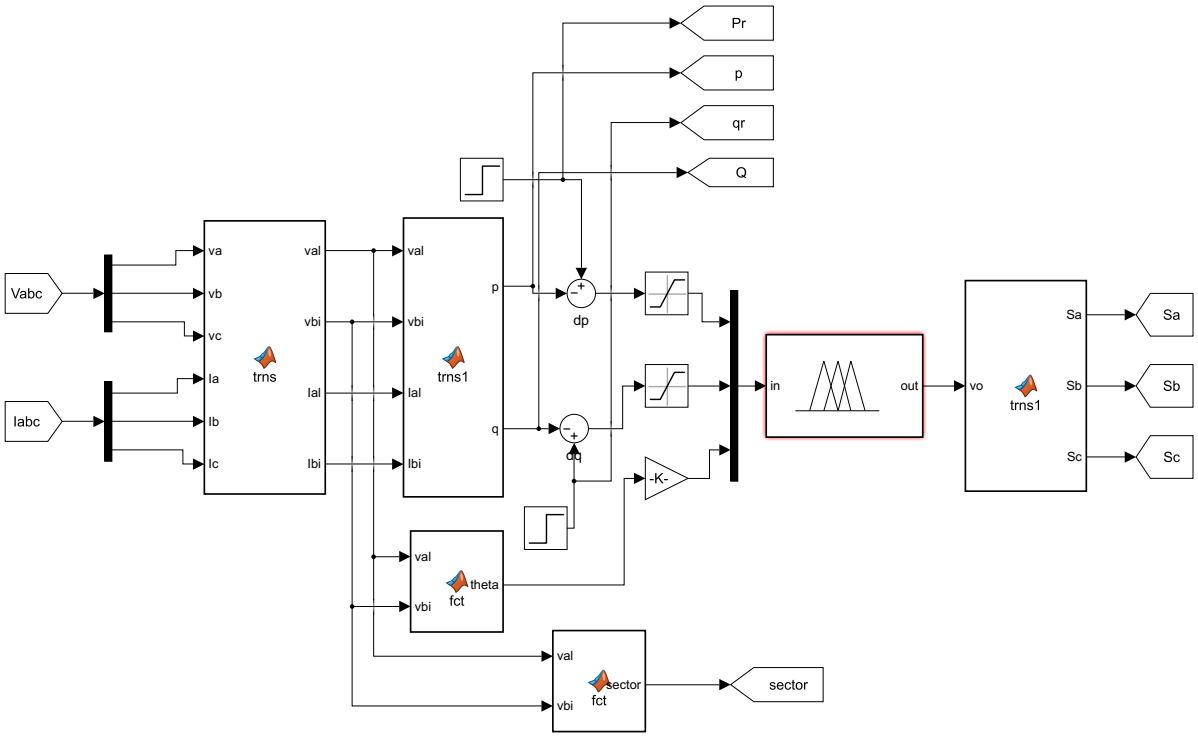

Figure 2.3: Structure of fuzzy direct power controller (FDPC)

The figure 2.4 shows that we have 2 member ship function for Δp and Δq six member ship function to design the 6 sectors, the output has 6 crisp values of Vi

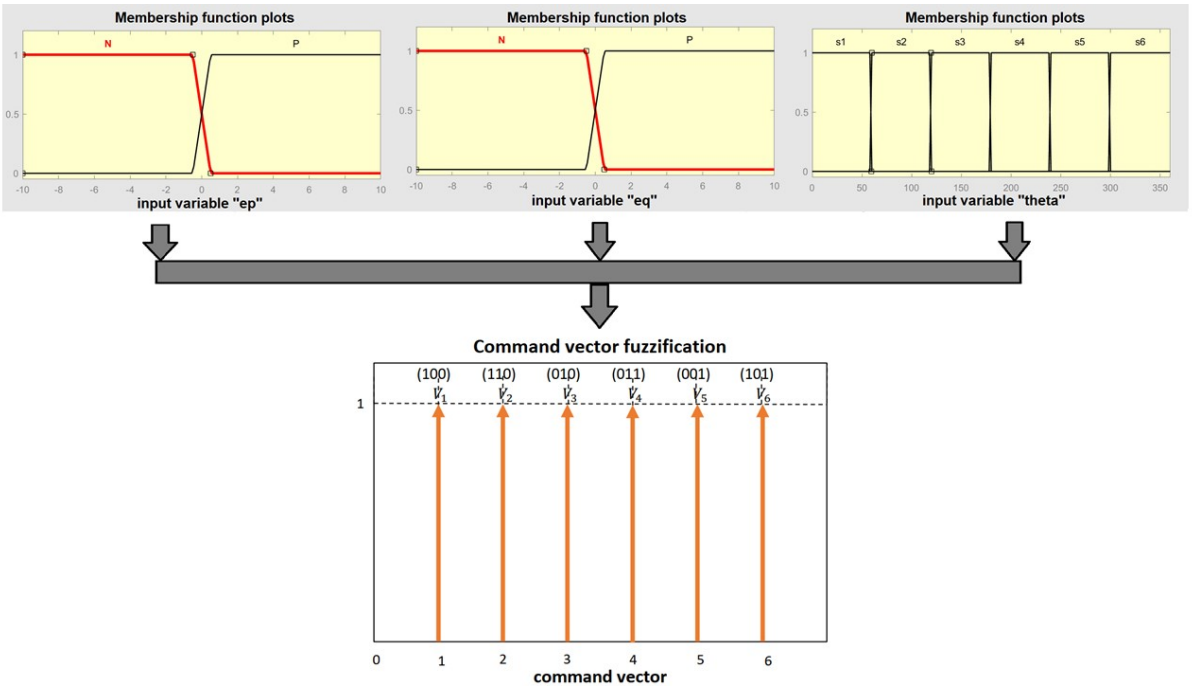

Figure 2.4: Fuzzification of inputs/outputs 6 sectors

The tables below represent Rule Inference systems used for both FDPC 6 sectors proposed by Eloy Garcia and Bouafia.

Table 2.1: Inference table 6-sector for FDPC proposed by Eloy-Garcia

Δp	Δq	S_1	S_2	S_3	S_4	S_5	S_6
N	N	v_5	v_6	v_1	v_2	v_3	v_4
N	P	v_3	v_4	v_5	v_6	v_1	v_2
P	N	v_1	v_2	v_3	v_4	v_5	v_6
P	P	v_2	v_3	v_4	v_5	v_6	v_1

Example of rules:
If Δp is N and Δq is N and S is S_1 then Vi=v_5.

Table 2.2: Inference table 6-sector for FDPC proposed by Bouafia

Δp	Δq	S_1	S_2	S_3	S_4	S_5	S_6
N	N	v_6	v_1	v_2	v_3	v_4	v_5
N	P	v_4	v_5	v_6	v_1	v_2	v_3
P	N	v_1	v_2	v_3	v_4	v_5	v_6
P	P	v_2	v_3	v_4	v_5	v_6	v_1

Example of rules:
If Δp is N and Δq is N and S is S_1 then Vi=v_6.

There are 24 rules for both switching algorithms. Figure 2.5 illustrate the fuzzy distribution surface for both 6 sector FDPC and figure 2.6 and 2.7 gives an examples of deffuzzification for a set of inputs $[\Delta q, \Delta p, \theta]$=[2,3,220°] and $[\Delta q, \Delta p, \theta]$=[0,0,180°].

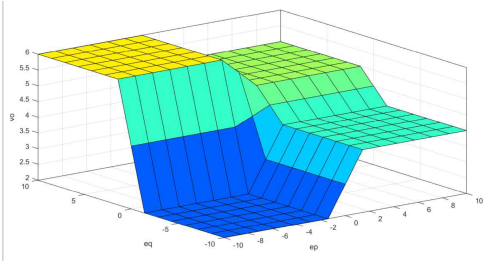

(a) Speech surface distribution 6-sector DPC proposed by Eloy-Garcia et al.

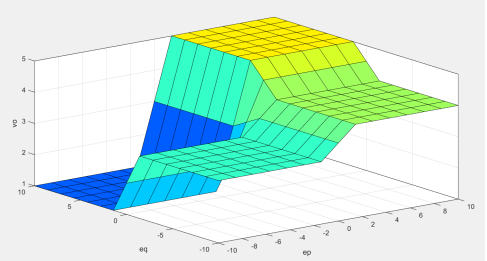

(b) Speech surface distribution 6-sector DPC prposed by Bouafia et al.

Figure 2.5: Fuzzy distribution surfaces for 6 sector algorithms

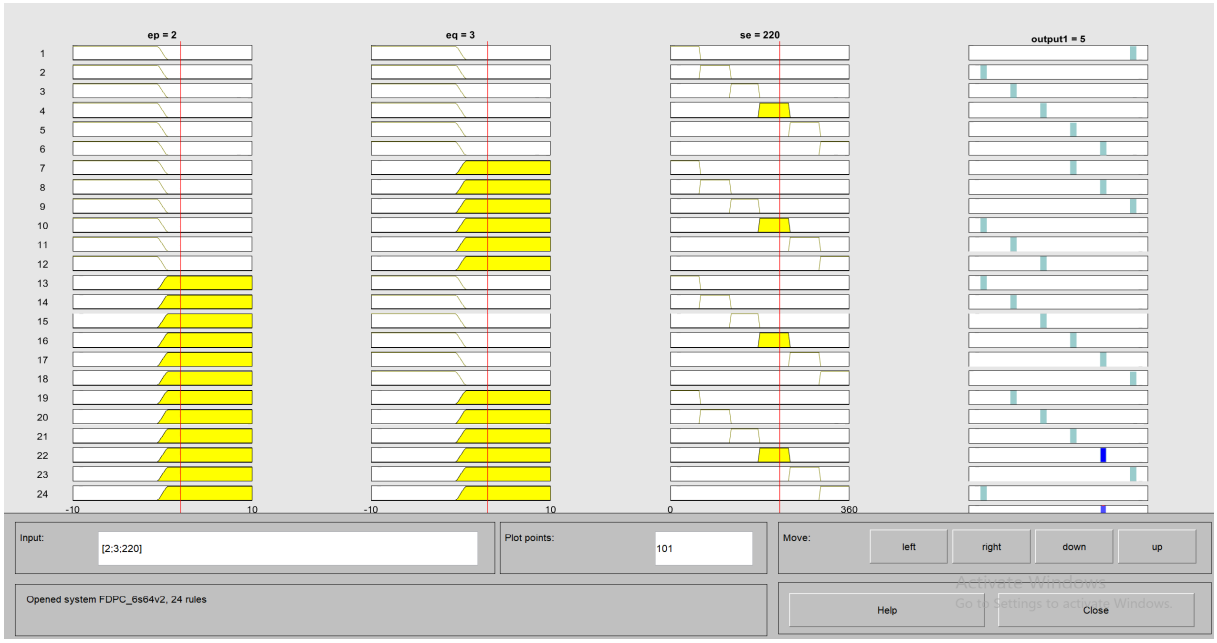

Figure 2.6: Rule Inference DPC 6-sector proposed by Bouafia et al. for $[\Delta q, \Delta p, \theta]$=[2,3,220°].

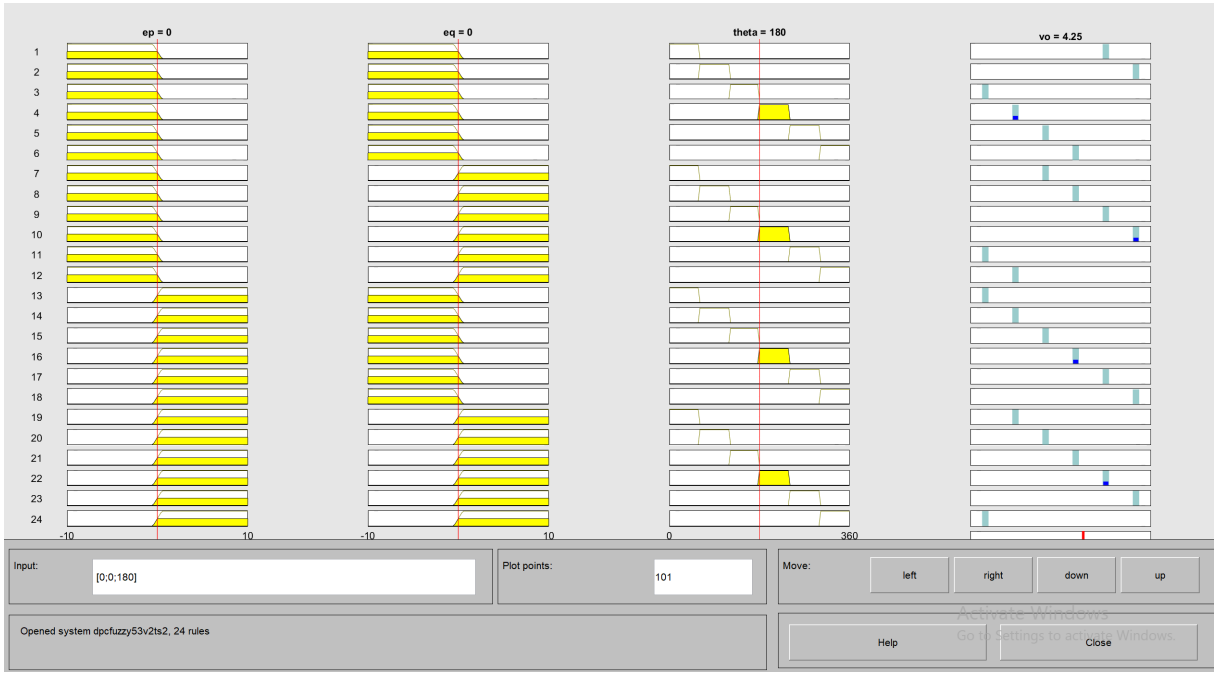

Figure 2.7: Rule Inference DPC 6-sector proposed by Eloy-Garcia and Alves $[\Delta q, \Delta p, \theta]$=[0,0,180°]

2.5.2 Development of fuzzy controllers to control for DPC 12-sector

The figure 2.2 steel the same in this approach withe the difference of sectors are 12 instead of the fuzificatiom of output will be Vi [V0, V1, V2, v3, V4, V5, V6, V7]. The 2 zero voltage vectors will be applied in this approach for both 12 sectors algorithm Vo and V7 for DPC 12-sector proposed by Nugoshi et al. and Baktash et al.

The figure 2.6 shows that we have three membership functions for eq and ep, and a 12 membership for theta for output voltage vector. We have eight crisp output vi i=0,...7.

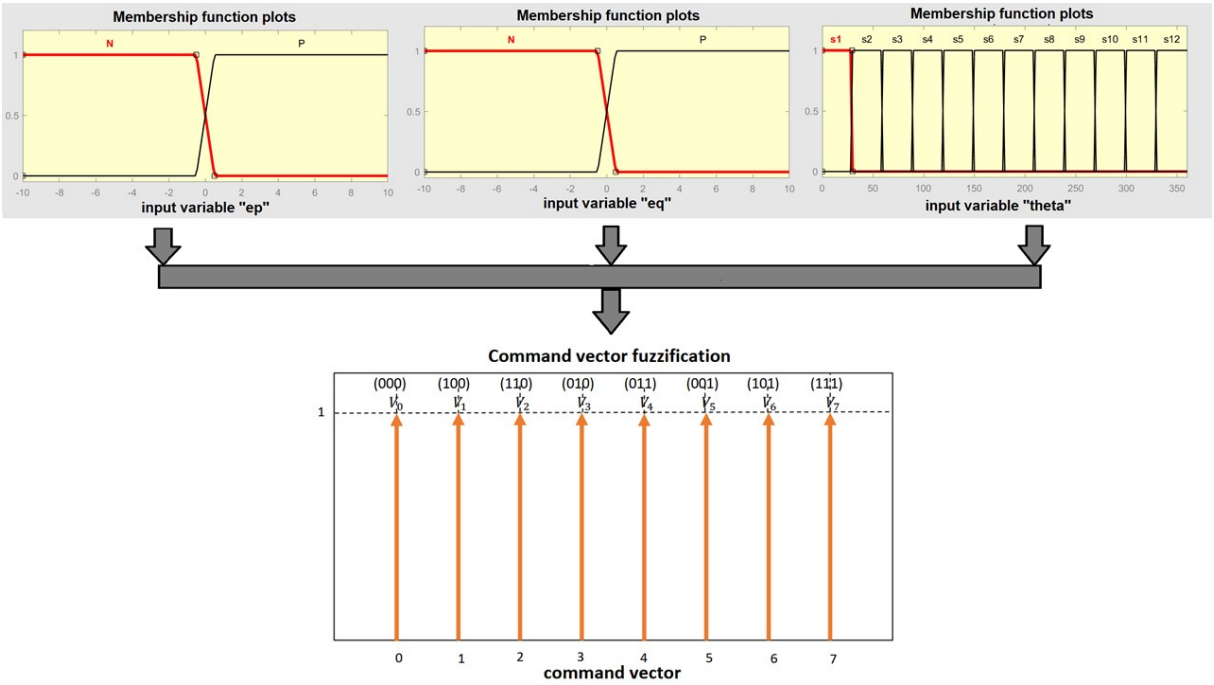

Figure 2.8: Fuzzification of inputs/outputs 12 sector

The tables below represent Rule Inference system used for both 12 sector FDPC proposed by Nugoshi et al. and Baktash et al.

Table 2.3: Inference table 12 sector DPC prposed by Baktash et al.

Δp	Δ_q	S_1	S_2	S_3	S_4	S_5	S_6	S_7	S_8	S_9	S_{10}	S_{11}	S_{12}
N	N	v_6	v_6	v_1	v_1	v_2	v_2	v_3	v_3	v_4	v_4	v_5	v_5
N	P	v_7	v_0	v_0	v_7	v_7	v_0	v_0	v_7	v_7	v_0	v_0	v_7
P	N	v_1	v_1	v_2	v_2	v_3	v_3	v_4	v_4	v_5	v_5	v_6	v_6
P	P	v_2	v_2	v_3	v_3	v_4	v_4	v_5	v_5	v_6	v_6	v_1	v_1

example of rules ;
If Δp is N and Δq is N and S is S1 than Vi is $v1$.

There is 48 rules for both switching algorithms. Figure 2.9 illustrate the fuzzy distribution surface for both 12 sector FDPC and figure 2.10 and 2.11 gives an examples of deffuzzification for a set of inputs $[\Delta q, \Delta p, \theta]$=[-2,5,100°] and $[\Delta q, \Delta p, \theta]$=[0,0,180°].

Table 2.4: Inference table DPC of 12-sector proposed by Nugoshi et al.

Δp	Δ_q	S_1	S_2	S_3	S_4	S_5	S_6	S_7	S_8	S_9	S_{10}	S_{11}	S_{12}
N	N	v_7	v_1	v_0	v_2	v_7	v_3	v_0	v_4	v_7	v_5	v_0	v_6
N	P	v_7	v_0	v_0	v_7	v_7	v_0	v_0	v_7	v_7	v_0	v_0	v_7
P	N	v_1	v_1	v_2	v_2	v_3	v_3	v_4	v_4	v_5	v_5	v_6	v_6
P	P	v_2	v_2	v_3	v_3	v_4	v_4	v_5	v_5	v_6	v_6	v_1	v_1

example of rules ;
If Δp is N and Δq is N and S is S1 than Vi is V7 there are 48 rules for both Switching algorithm

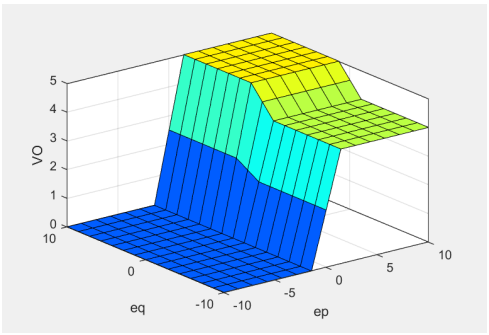

(a) Speech surface distribution 12-sector proposed by Nugoshi et al

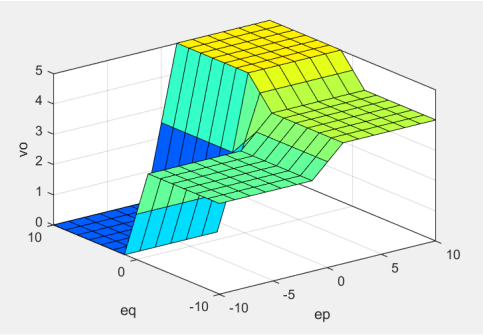

(b) Speech surface 12-sector proposed by Baktash et al

Figure 2.9: Fuzzy distribution surfaces for 12 sector algorithms

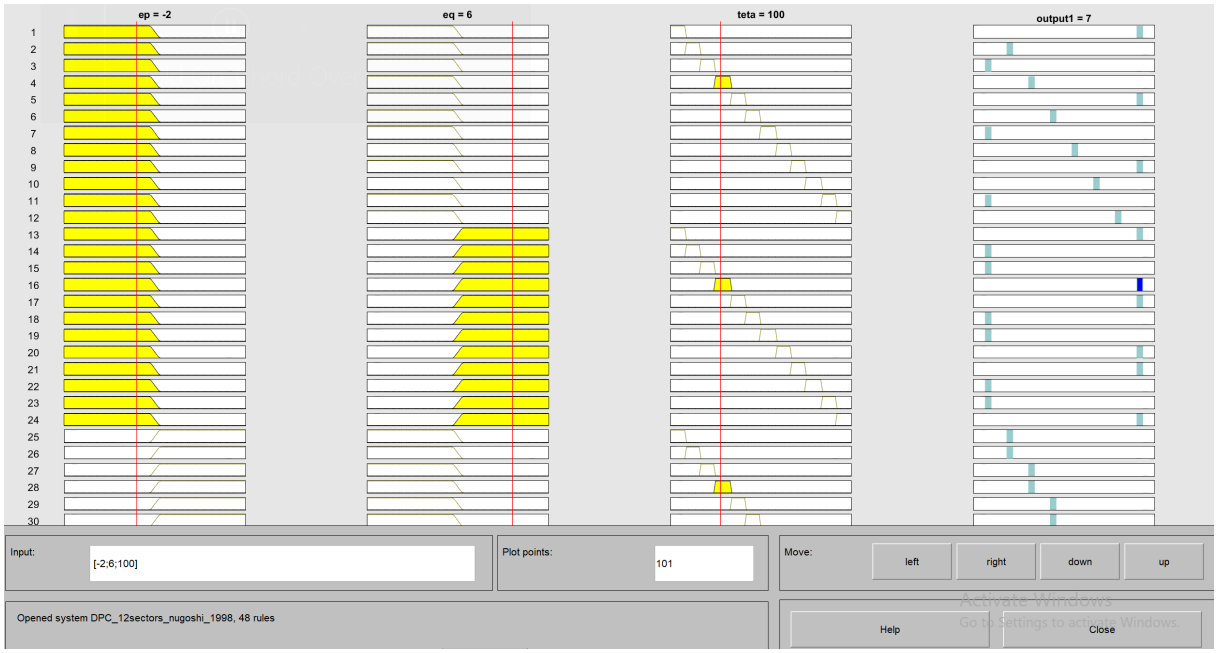

Figure 2.10: Rule InferenceDPC 12-sector proposed by Nugoshi et al for $[\Delta q, \Delta p, \theta]$=[-2,6,100°]

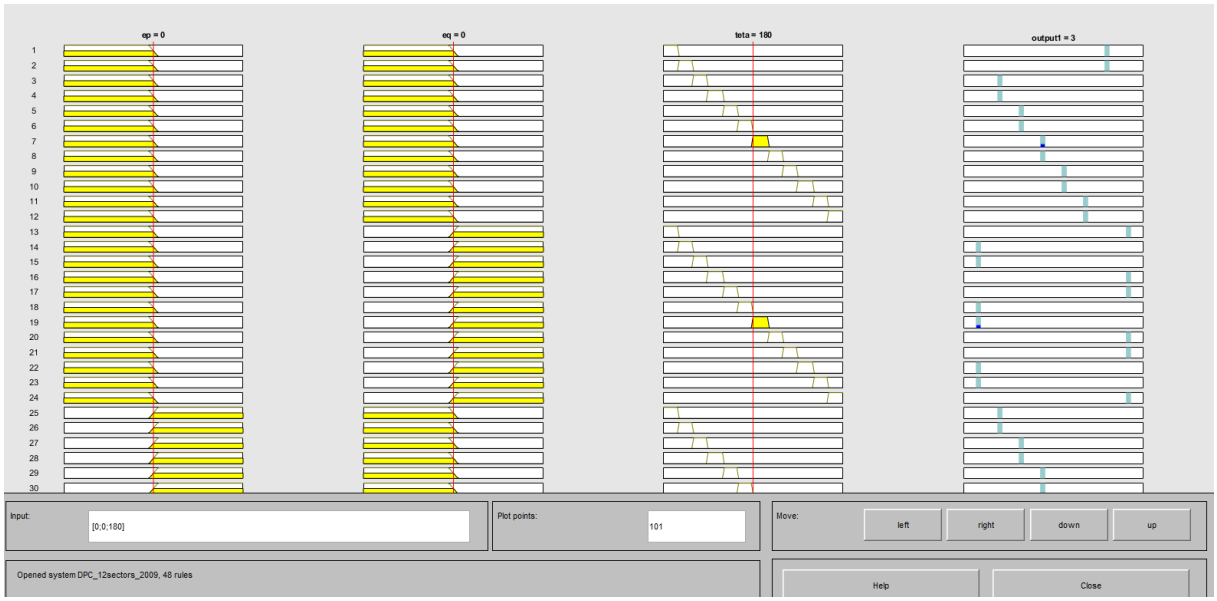

Figure 2.11: Rule Inference 12-sector proposed by Baktash et al for $[\Delta q, \Delta p, \theta]$=[0,0,180°]

2.6 Conclusion

In this chapter, we presented the theory of fuzzy logic, in addition to the various basic concepts of this technique. We have replaced the classical controllers based on Switching table and Hysteresis controller with a fuzzy controllers in which we have used fuzzy logic principles in order to improve the static and dynamic performance of classical DPC.

Chapter 3

Comparative Study between Classic DPC and DPC developed with Fuzzy Logic

3.1 Introduction

This chapter presents a comparative analysis of two distinct power control techniques: conventional direct power control (DPC) fuzzy-based direct power control (FDPC). Fuzzy logic control (FLC) introduces an intelligent approach that addresses the inherent nonlinearity and uncertainty in power control systems. By employing a set of linguistic rules and membership functions, FLC mimics human reasoning, enabling effective decision-making in control processes. The study aims to provide a comprehensive understanding of the strengths and limitations of classic DPC and FDPC offering insights into their practical applications and potential improvements in power control.

3.2 Simulation model

To verify the efficiency of a two-level inverter connected to the grid using the Fuzzy-based direct power control FDPC, the simulation model presented in Figure (3.1) is chosen. This model contains the following elements: constant voltage sources, a two-level inverter, an RL connection filter, a three-phase current and voltage measuring block, a direct power control, and a three-phase electrical grid. The simulation model structure of DPC is presented in Figure 3.2, while the simulation model structure of FDPC is illustrated in Figure 3.3. These models are specifically chosen to facilitate the comprehensive evaluation of the FDPC's performance in controlling the power flow between the two-level inverter

and the grid.

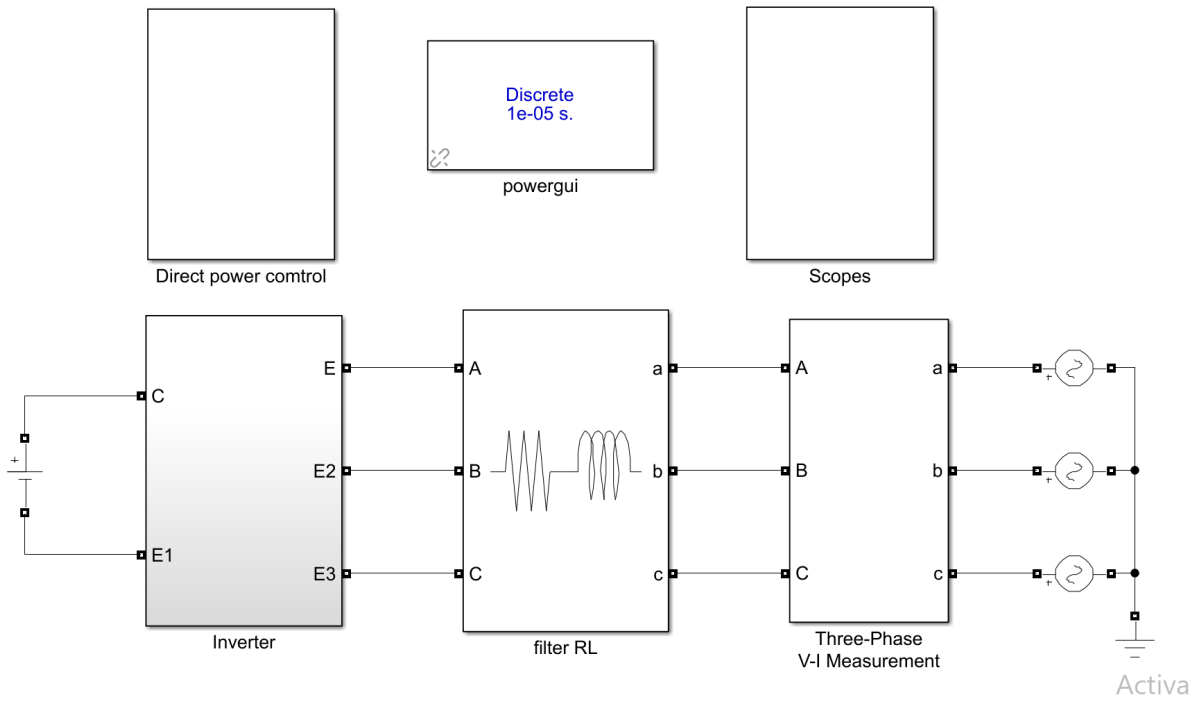

Figure 3.1: Simulink model for two-level grid-connected inverter

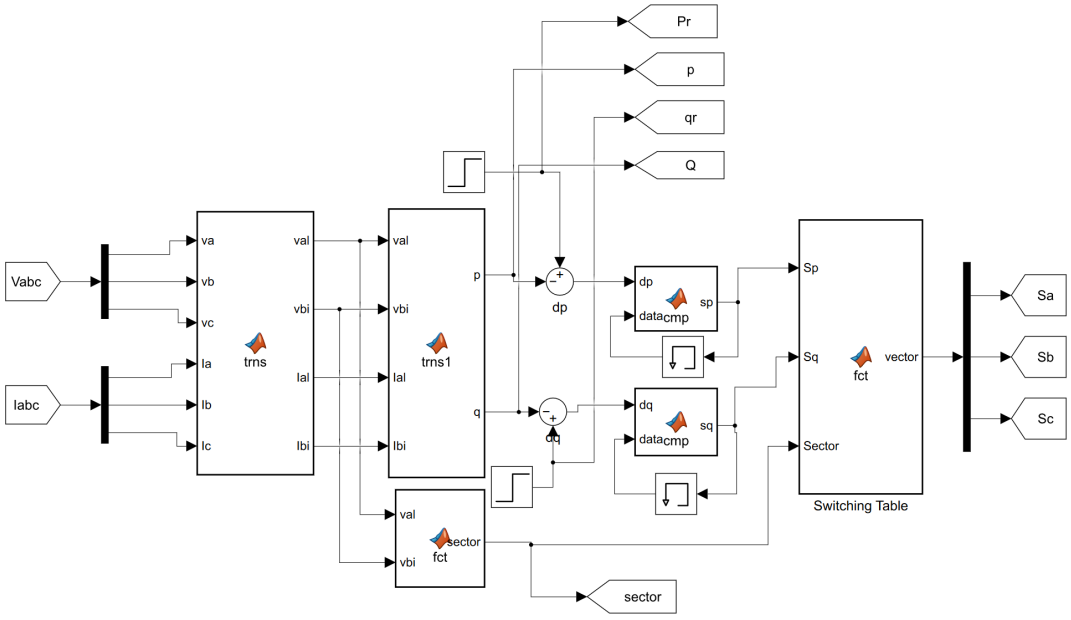

Figure 3.2: Structure of direct power controller (DPC)

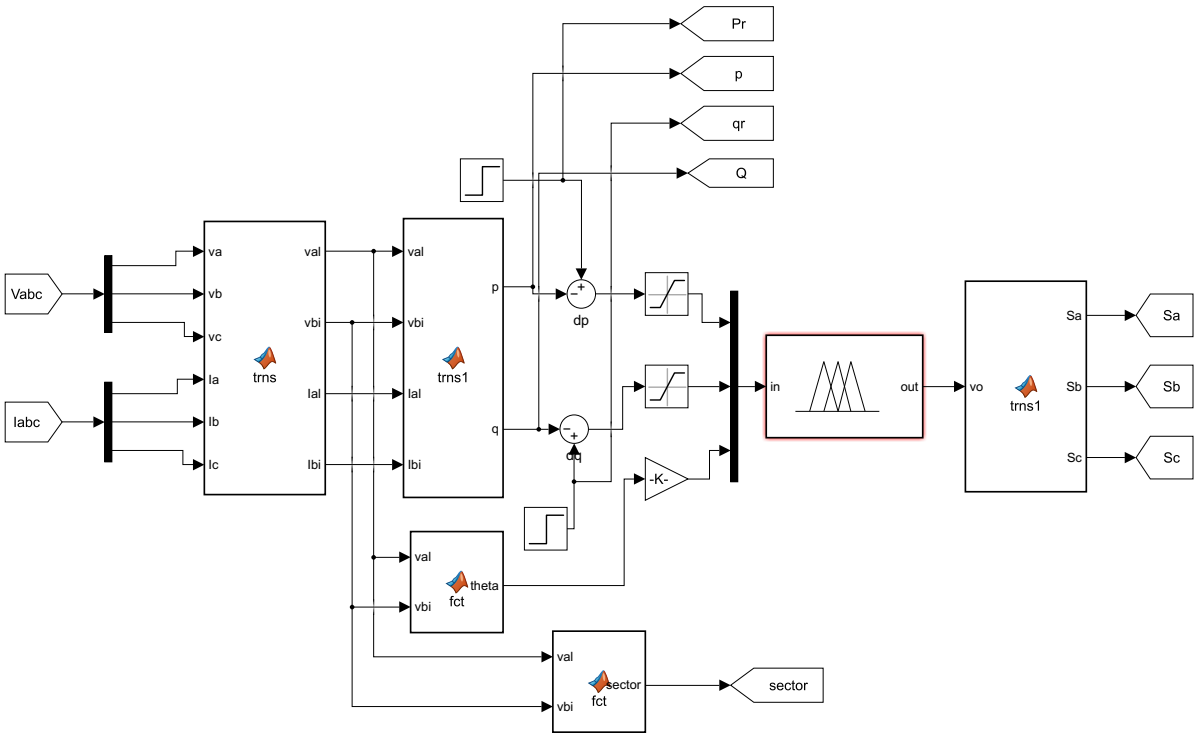

Figure 3.3: Structure of fuzzy direct power controller (FDPC)

3.3 Results and interpretation

3.3.1 Steady-state operation

Figure 1.11 illustrated the results of 6-sector, 12-sector, and three-phase voltages Vabc, while figures 3.4, 3.6, 3.8 and 3.10 illustrate the simulation results of the two-level grid-connected inverter for 6 and 12 sector, including reactive power (q), active power (p), reactive power reference (qr), and active power reference (pr), grid voltage Va and line current Ia, line currents (Iabc). Furthermore, figure 3.5, 3.7, 3.9, and 3.11 represent the Total Harmonics Distortion THD of the line current Ia.

In both DPC and FDPC with constant Pr and Qr, the currents (Ia) and voltages (Va) are in-phase indicting a stable and aligned phase relationship between current and voltage. This synchronization occurs due to the absence of sudden changes in reactive power (qr), which would otherwise introduce phase shifts.

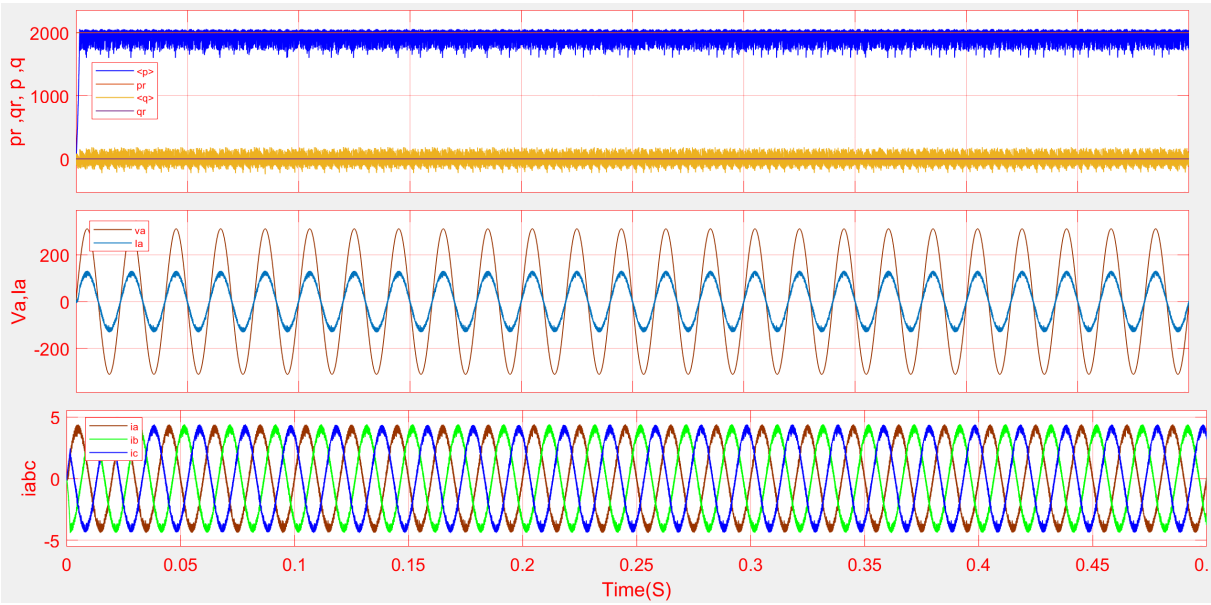

Figure 3.4: Simulation results of the active and reactive powers (pr, p, qr, q), line currents (Iabc, Ia), grid voltage (va) for DPC using switching table proposed by Eloy-Garcia and Alves under steady-state operation with p=2000W and q=0Var.

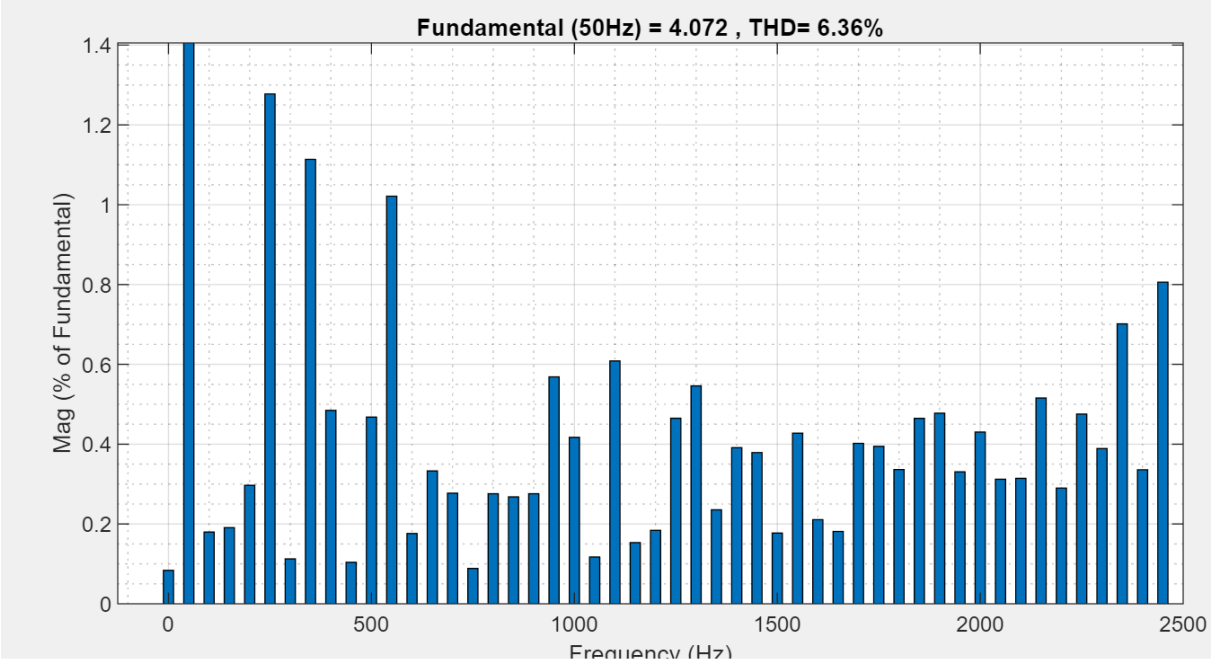

Figure 3.5: THD result of line current for DPC using switching table proposed by Eloy-Garcia and Alves under steady-state operation with p=2000W and q=0Var.

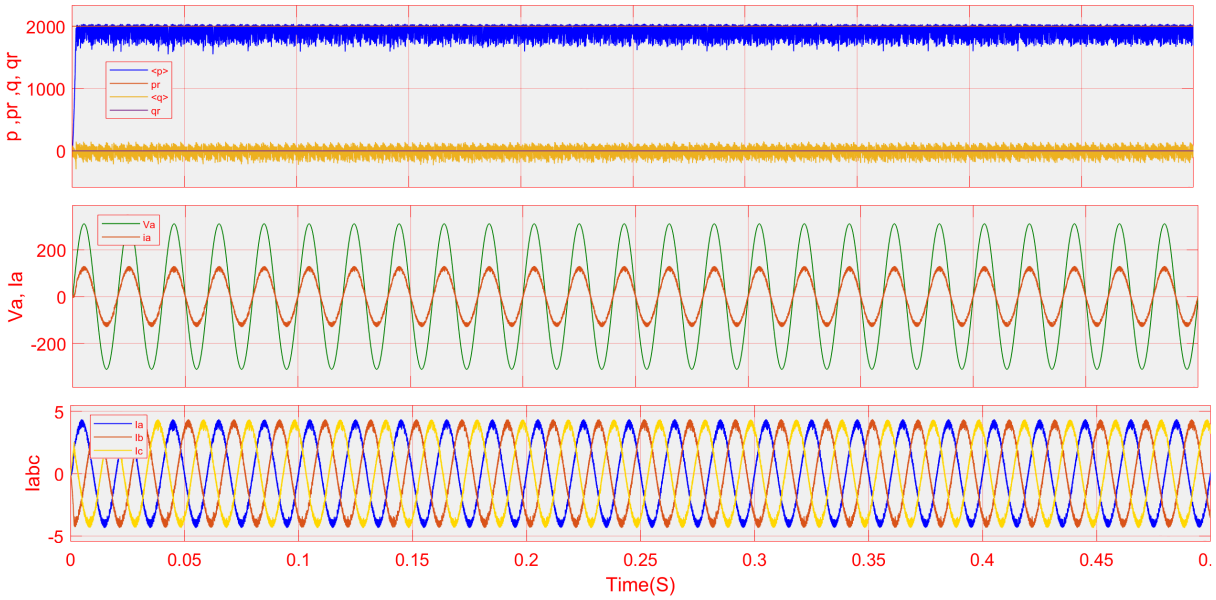

Figure 3.6: Simulation results of the active and reactive powers (pr, p, qr, q), line currents (Iabc, Ia), grid voltage (va) for FDPC using switching table proposed by Eloy-Garcia and Alves under steady-state operation with p=2000W and q=0Var.

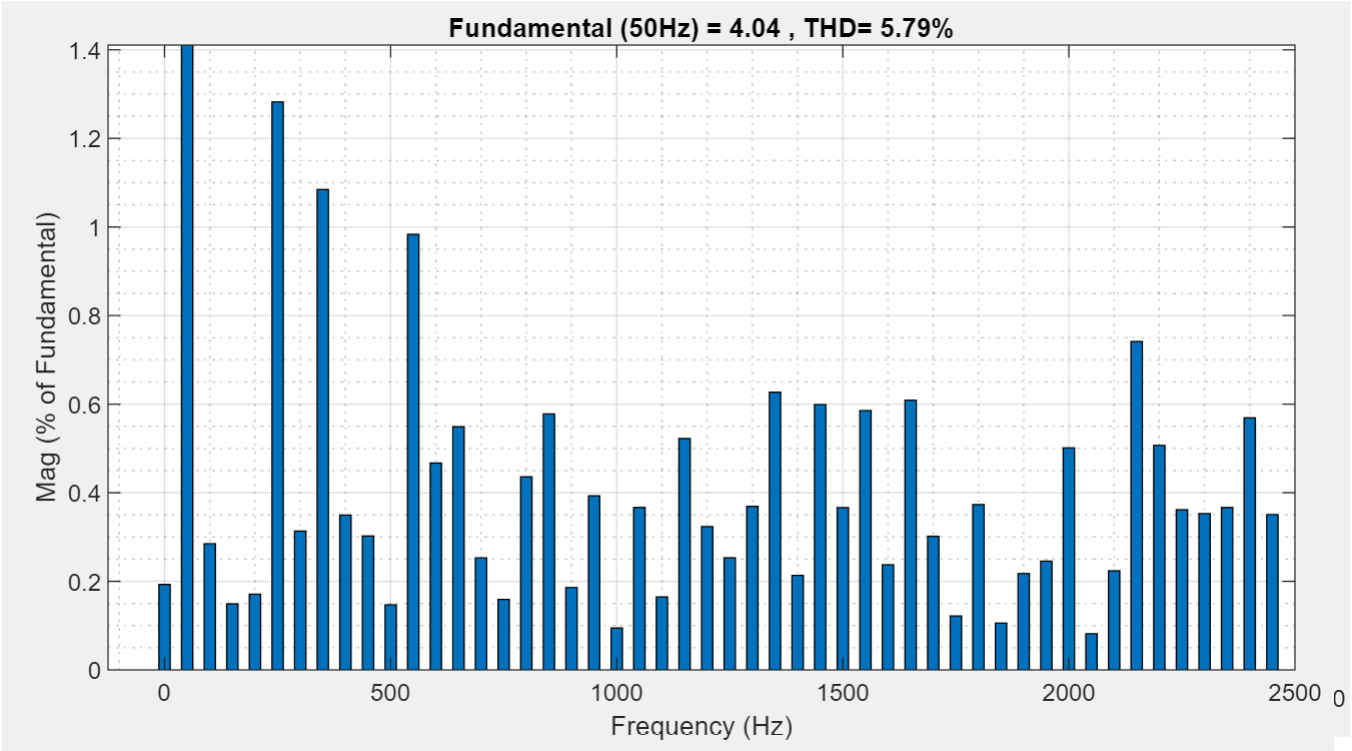

Figure 3.7: THD result of line current for FDPC using switching table proposed by Eloy-Garcia and Alves under steady-state operation with p=2000W and q=0Var.

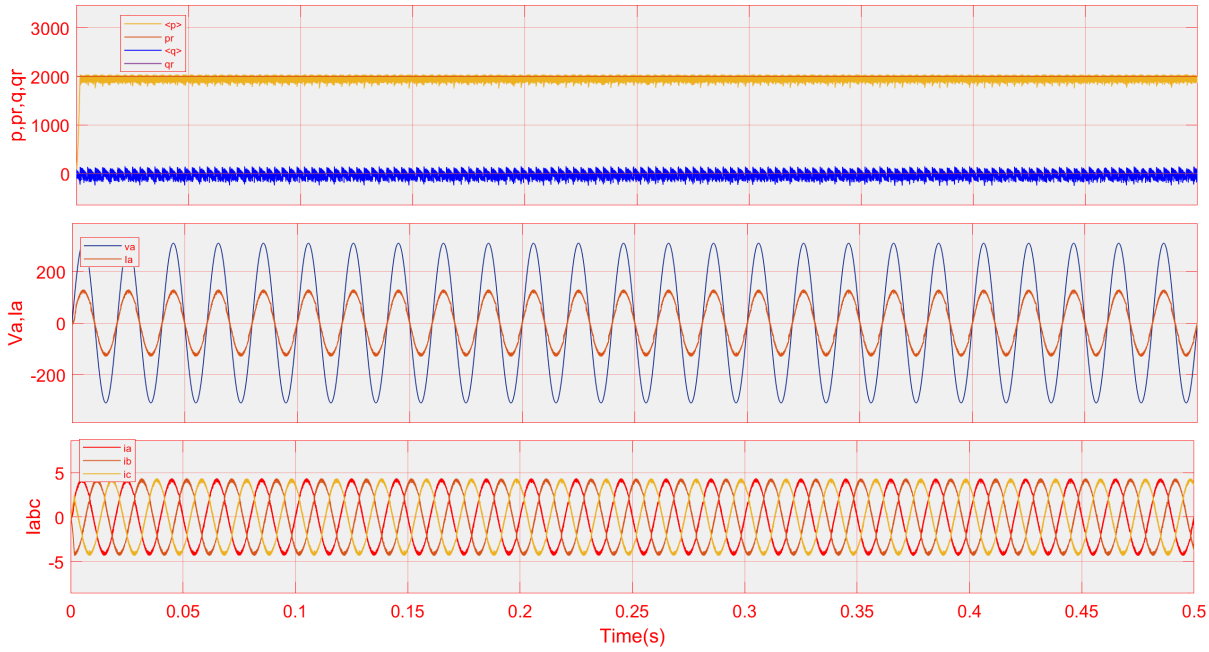

Figure 3.8: Simulation results of the active and reactive powers (pr, p, qr, q), line currents (Iabc, Ia), grid voltage (va) for DPC using switching table proposed by Baktash et al. under steady-state operation with p=2000W and q=0Var.

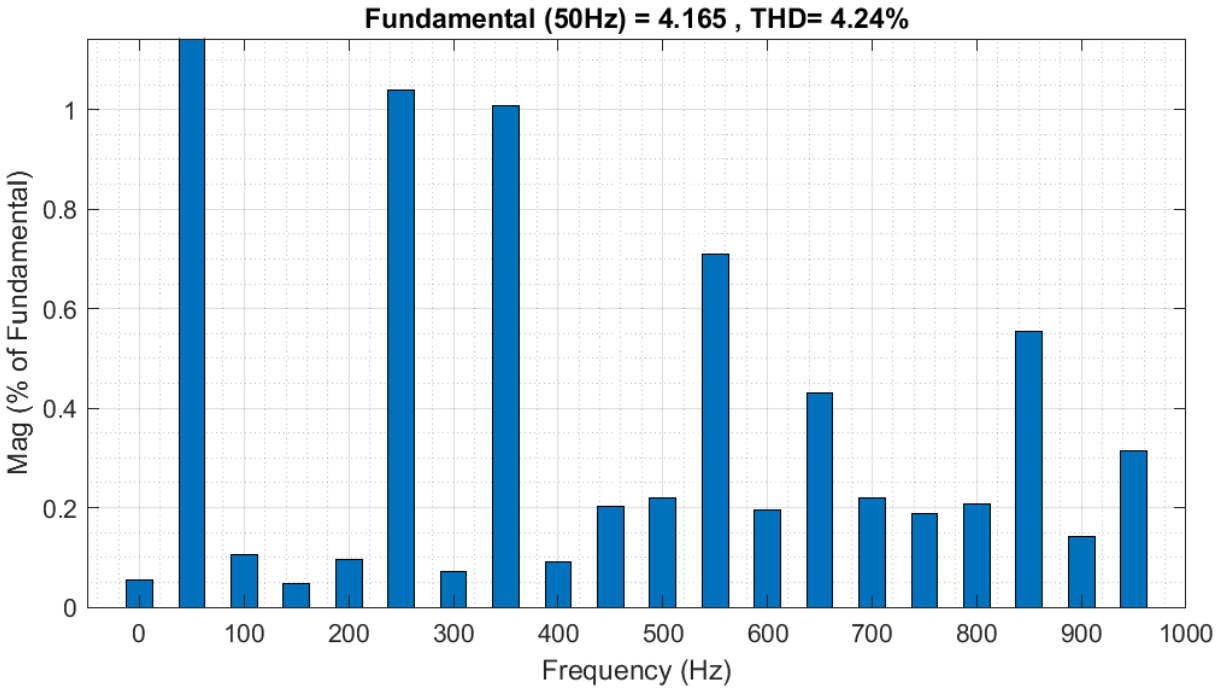

Figure 3.9: THD result of line current for DPC using switching table proposed by Baktash et al. under steady-state operation with p=2000W and q=0Var.

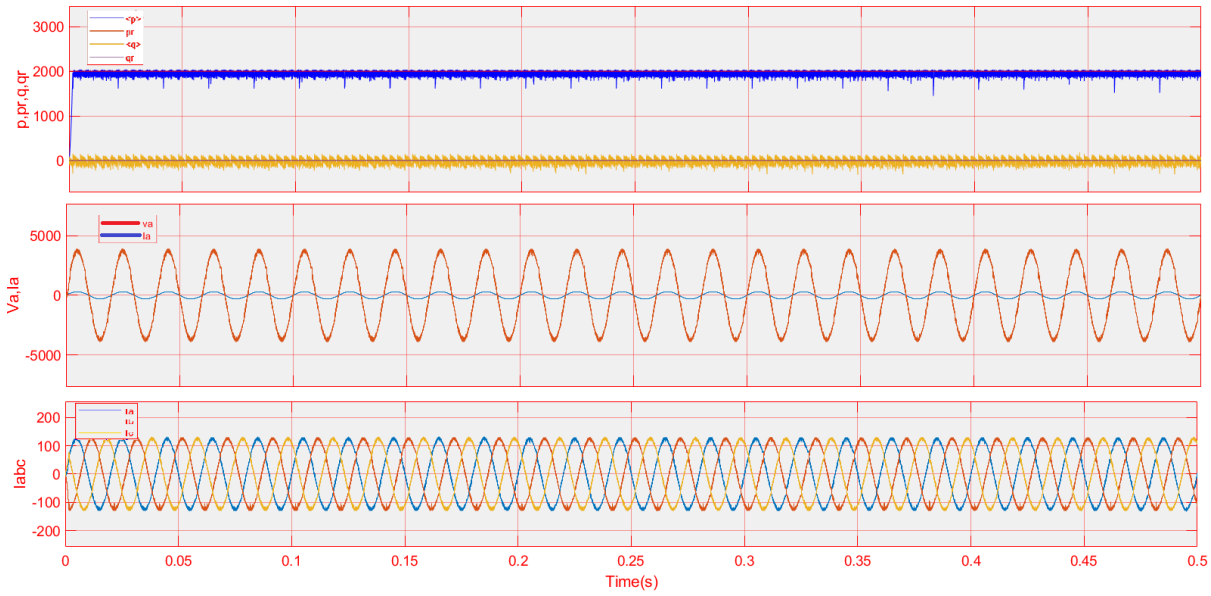

Figure 3.10: Simulation results of the active and reactive powers (pr, p, qr, q), line currents(Iabc, Ia), grid voltage (va) for FDPC using switching table proposed by Baktash et al. understeady-state operation with p=2000W and q=0Var.

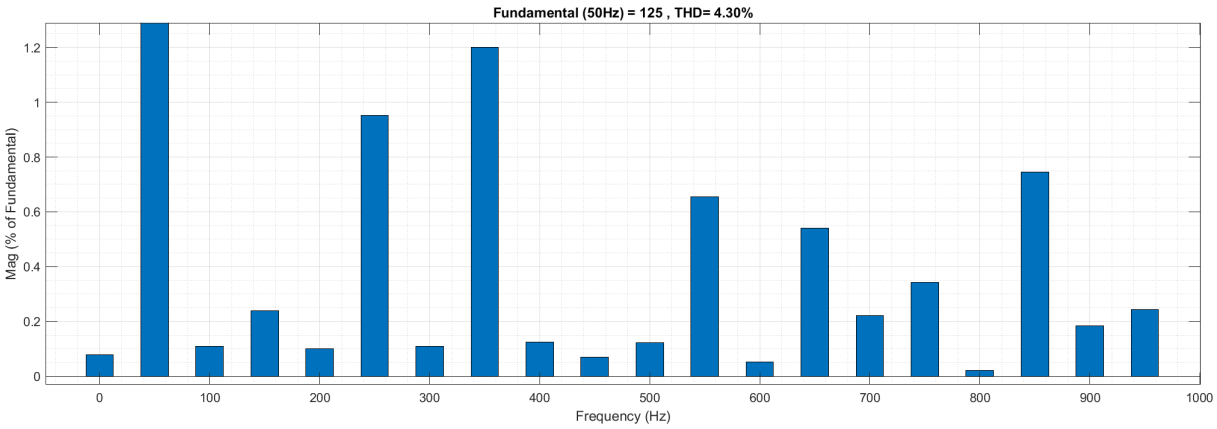

Figure 3.11: THD result of line current for FDPC using switching table proposed by Baktash et al. under steady-state operation with p=2000W and q=0Var.

3.3.2 Active and Reactive power variation

Figures 3.12, 3.14, 3.16 and 3.18 illustrate the simulation results of the two-level grid-connected inverter for 6 and 12 sector, including reactive power (q), active power (p), reactive power reference (qr), and active power reference (pr), grid voltage Va and line current Ia, line currents (Iabc). Furthermore, figures 3.13, 3.15, 3.17 and 3.19 represent the total harmonics distortion THD of the line current Ia.
In both DPC and FDPC schemes, pr and qr variations were introduced. The pr was stepped from 1000W initially, to 2000W at t=0.2s, and then to 3000W at t=0.4s. Similarly, the qr was varied from 0VAR initially, to 500VAR at t=0.3s, and 1000VAR at t=0.4s. It was observed that the current (Ia) and voltage (Va) were not in phase after t=0.3s when the reactive power changed to 500VAR. Additionally, the line currents (Iabc) exhibited incremental changes corresponding to the active power variations, with the magnitude of Iabc changing in the same direction as the active power.

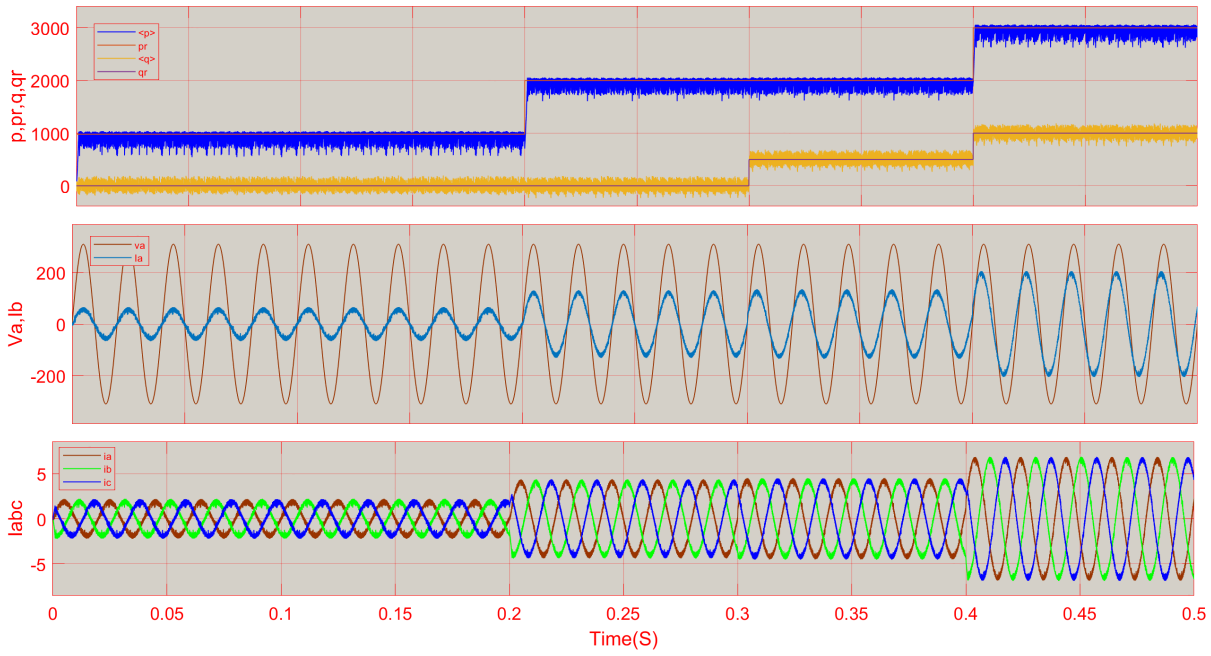

Figure 3.12: Simulation results of the active and reactive powers (pr, p, qr, q), line currents (Iabc, Ia), grid voltage (va) for DPC using switching table proposed by Eloy-Garcia and Alves under active and reactive powers variation.

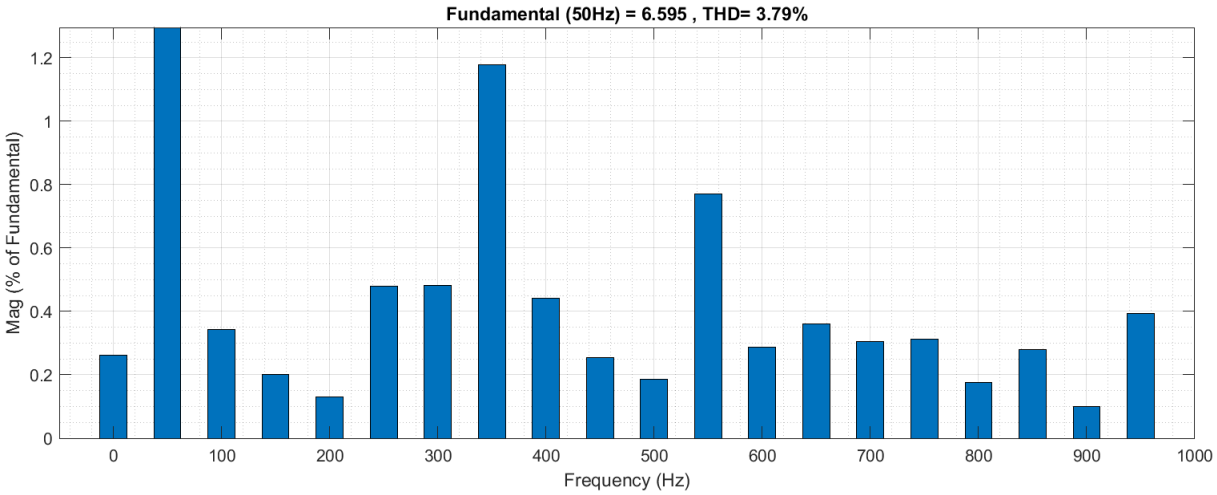

Figure 3.13: THD result of line current for DPC using switching table proposed by Eloy-Garcia and Alves under active and reactive powers variation.

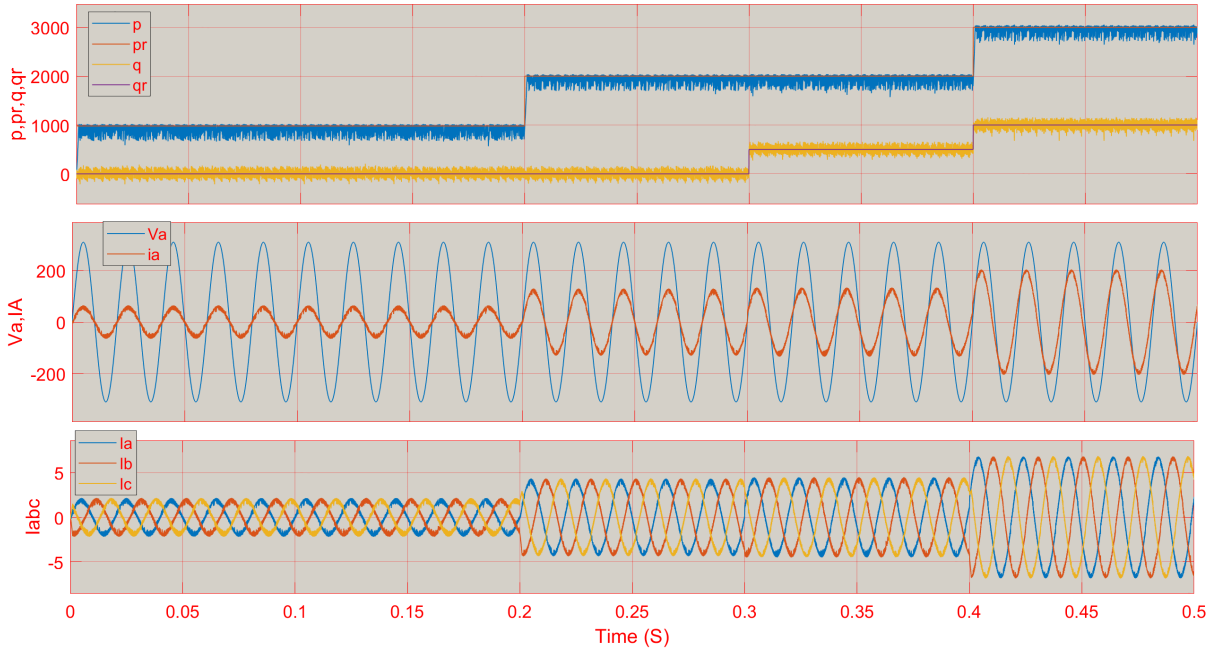

Figure 3.14: Simulation results of the active and reactive powers (pr, p, qr, q), line currents (Iabc, Ia), grid voltage (va) for FDPC using switching table proposed by Eloy-Garcia and Alves under active and reactive powers variation.

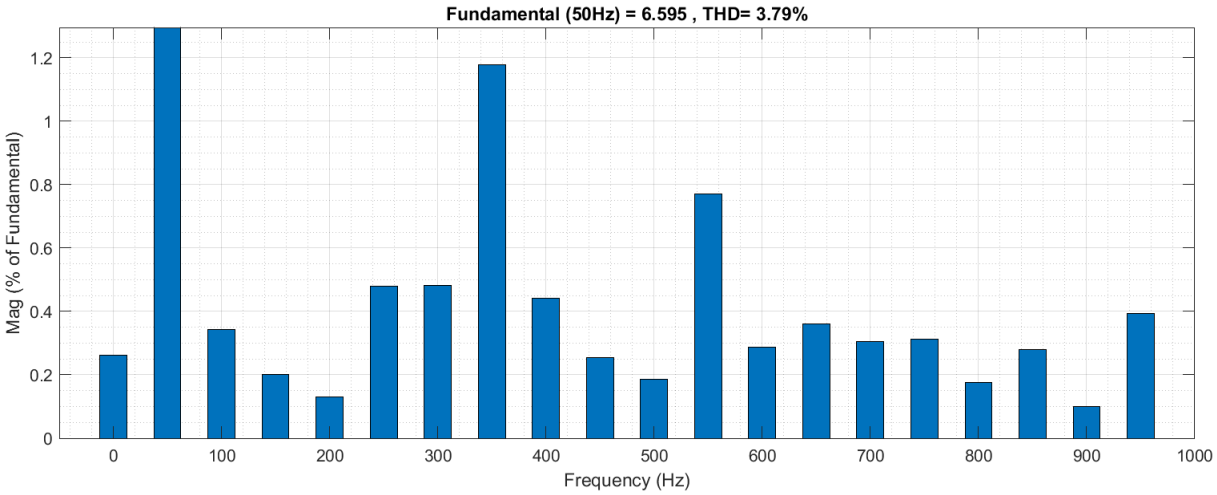

Figure 3.15: THD result of line current for FDPC using switching table proposed by Eloy-Garcia and Alves under active and reactive powers variation.

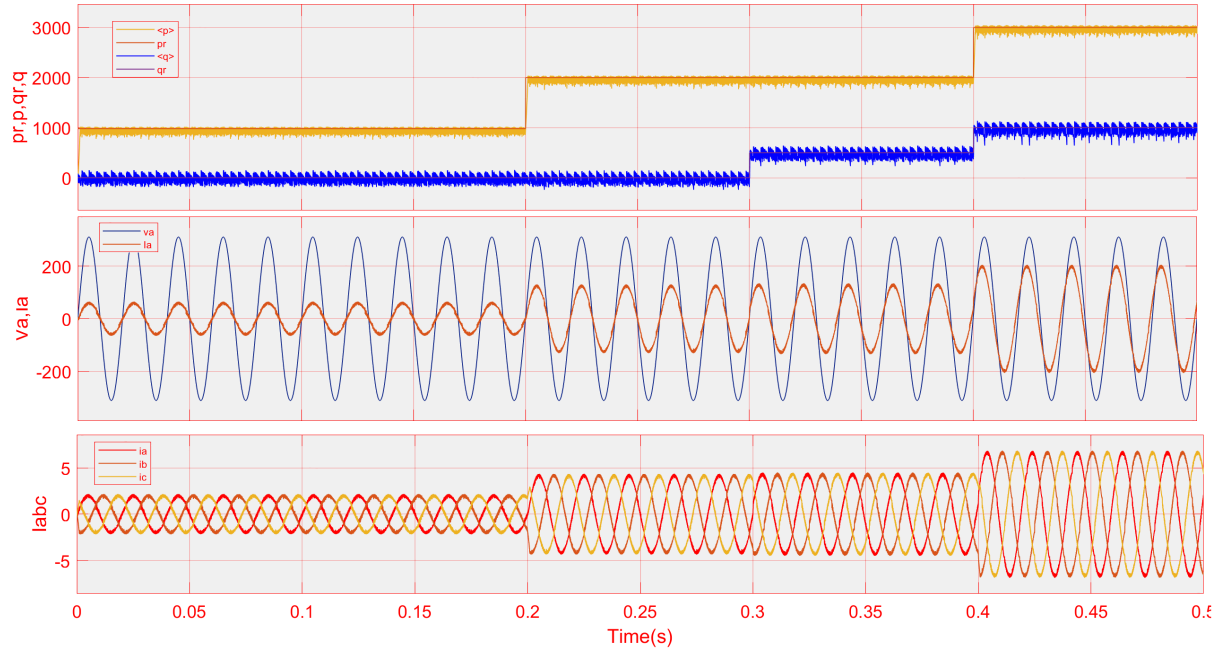

Figure 3.16: Simulation results of the active and reactive powers (pr, p, qr, q), line currents (Iabc, Ia), grid voltage (va) for DPC using switching table proposed by Baktash et al. under active and reactive powers variation.

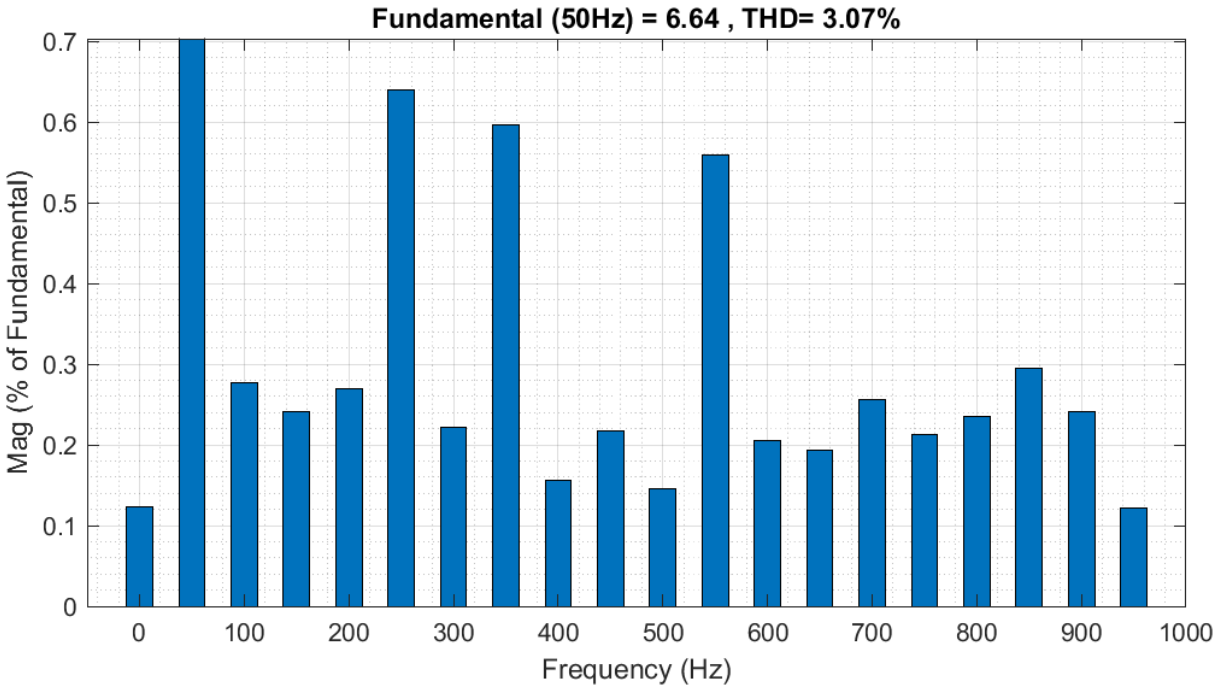

Figure 3.17: THD result of line current for DPC using switching table proposed by Baktash et al.under active and reactive powers variation.

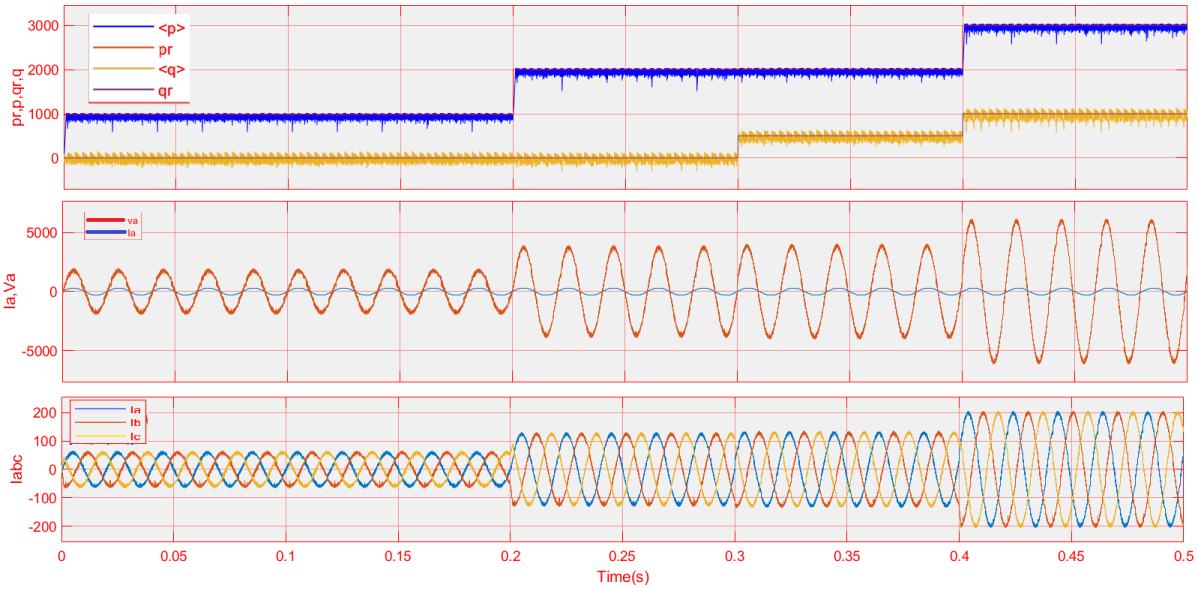

Figure 3.18: Simulation results of the active and reactive powers (pr, p, qr, q), line currents (Iabc, Ia), grid voltage (va) for FDPC using switching table proposed by Baktash et al. under active and reactive powers variation.

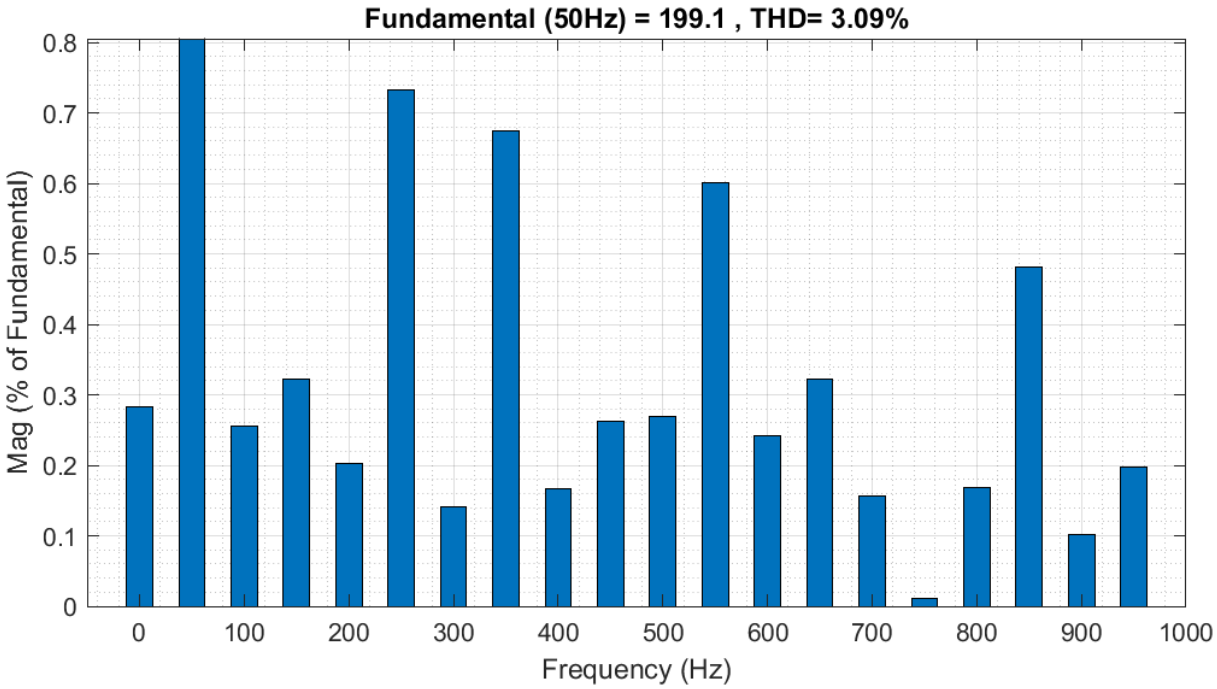

Figure 3.19: THD result of line current for FDPC using switching table proposed by Baktash et al. under active and reactive powers variation.

3.3.3 Sampling time variation

Table 3.1 presents the total harmonic distortion (THD) results of the line current (Ia) for both DPC and FDPC power control in a two-level grid-connected inverter with 6 and 12 sectors. In this control schemats, variations in the sampling time (Ts) were introduced, ranging from 1 $\mu sto12\mu s$.

It was observed that as the sampling time increased, indicating higher distortion levels. This highlights the influence of sampling time on the current quality, witch consequently affects the active and reactive powers control performance.

Table 3.1: THD of line current for DPC and FDPC techniques using switching tables proposed by Eloy-Garcia Alves and Baktash et al. under varying sampling times

$T_s(\mu s)$	1	2	4	6	8	10	12
Eloy-Garcia DPC	1.01	1.37	2.04	2.65	3.37	3.95	4.40
Eloy-Garcia FDPC	0.82	0.74	1.43	1.99	2.57	3.33	3.95
Baktash DPC	1.16	1.35	1.64	1.99	2.74	2.99	3.62
Baktash FDPC	1.72	1.54	1.84	2.14	2.46	3.01	3.56

3.4 Conclusion

In this chapter, a Comparative analysis between the classical DPC and fuzzy-based DPC was presented. This analysis was based on simulation tests of two-level grid-connected inverter employing DPC and FDPC strategies.

From the simulation results, the active and reactive powers accurately follow their respective reference values for both the switching tables utilized. The line current (Ia) and grid voltage (Va) remained in-phase due to the absence of sudden changes in reactive power (qr), which could otherwise introduce phase shifts. The FDPC with fuzzy logic in 6 sectors demonstrated improved performance compared to the classical switching tables discussed in the previous chapter. For the 12-sector case, the results were comparable between classical and fuzzy logic approaches. Hence, the fuzzy region played a crucial role in reducing the THD in the line current.

General Conclusion

In our final project, we presented a modeling and design of a grid-connected inverter system utilizing fuzzy logic control. The system comprised a two-level three-phase inverter controlled by direct power control (DPC) and fuzzy-based direct power control (FDPC) techniques.

Firstly, We conducted a detailed modeling and control study of a two-level grid-connected inverter system. This system consisted of a two-level inverter, a connection filter, and a grid interface. The two-level inverter was controlled using the conventional DPC method, which directly regulates active and reactive powers.

Secondly, We introduced the fuzzy logic principles and developed a fuzzy logic-based DPC (FDPC) technique. This approach replaced the switching table and hysteresis comparators used in conventional DPC with a fuzzy logic controller.

Finaly, we performed a comparative analysis between the conventional DPC and the proposed FDPC methods through matlab/simulink simulations of the two-level grid-connected inverter system. This analysis evaluated the performance and efficacy of the two-control strategies.

From the simulation results obtained, we found that:

- The active and reactive powers perfectly follow their reference values for the two controls.

- Varying the active power makes it possible to increase or decrease the line current. As well as, the variation of the reactive power makes it possible to advance or delay the line current.

- The increase in the sampling period including an increase in the THD values for both conventional DPC and fuzzy-based DPC commands.

- The FDPC can dynamically adjust to changes in system conditions, resulting in a faster and more accurate response to power fluctuations compared to the DPC.

- The inherent robustness of fuzzy logic allows the control system to maintain stable operation under a wide range of operating conditions.

- The FDPC does not require a precise mathematical model of the system, simplifying the design process and making it easier to implement in complex and uncertain environments.

- The use of fuzzy logic in DPC helps in reducing the THD in the current, leading to better power quality and compliance with grid standards.

Overall, integrating fuzzy logic into DPC for two-level grid-connected converters enhances the efficiency, reliability, and flexibility of power control, making it a promising solution for modern power electronics applications.

As future perspectives stemming from this dissertation work, it would be interesting to:

- Investigate the application of other artificial intelligence techniques, such as neural networks and fuzzy-neural networks for inverter control strategies.

- Extend the study to encompass other multilevel inverter topologies interfaced with electrical grids, utilizing the DPC algorithm.

- Undertake practical implementation and experimental validation of the proposed algorithms.

Bibliography

[1] Abdelouahab Bouafia, Jean-Paul Gaubert, and Fateh Krim. Analysis and design of new switching table for direct power control of three-phase pwm rectifier. In *2008 13th International Power Electronics and Motion Control Conference*, pages 703–709. IEEE, 2008.

[2] J Eloy-Garcia, S Arnaltes, and JL Rodriguez-Amenedo. Direct power control of voltage source inverters with unbalanced grid voltages. *IET Power Electronics*, 1(3):395–407, 2008.

[3] JG Norniella, JM Cano, GA Orcajo, CH Rojas, JF Pedrayes, MF Cabanas, and MG Melero. Optimization of direct power control of three-phase active rectifiers by using multiple switching tables. In *International Conference of Renewable Energies and Power Quality (ICREPQ'10)*, 2010.

[4] Zahrat Ennada MOGDAD and Abderahman LAKAB. Commande directe de puissance des convertisseurs multiniveaux à diodes flottantes connectés aux réseaux. Master's thesis, Université Kasdi Merbah ouargla, 2023.

[5] Tapan A Trivedi, Rajendrasinh Jadeja, and Praghnesh Bhatt. A review on direct power control for applications to grid connected pwm converters. *Engineering, Technology & Applied Science Research*, 5(4):841–849, 2015.

[6] A Fekik, H Denoun, AT Azar, ML Hamida, N Benamrouche, and S Vaidyanathan. Direct power control of a pwm-inverter for grid connected photovoltaic system. In *5nd international conference on renewable Energy (CIER2017)*, pages 20–22, 2017.

[7] Toshihiko Noguchi, Hiroaki Tomiki, Seiji Kondo, and Isao Takahashi. Direct power control of pwm converter wifout power-source voltage sensors. *IEEE transactions on industry applications*, 34(3):473–479, 1998.

[8] Sergio Vazquez, Juan Antonio Sanchez, Juan Manuel Carrasco, Jose Ignacio Leon, and Eduardo Galvan. A model-based direct power control for three-phase power converters. *IEEE Transactions on Industrial Electronics*, 55(4):1647–1657, 2008.

[9] Gerardo Escobar, Aleksandar M Stankovic, Juan M Carrasco, Eduardo Galván, and Romeo Ortega. Analysis and design of direct power control (dpc) for a three phase synchronous rectifier via output regulation subspaces. *IEEE Transactions on Power Electronics*, 18(3):823–830, 2003.

[10] Djaafer Lalili. *Mli vectorielle et commande non linéaire du bus continu des onduleurs multiniveaux*. PhD thesis, Alger, Ecole Nationale Supérieure Polytechnique, 2009.

[11] Bin Wu and Mehdi Narimani. Two-level voltage source inverter. 2017.

[12] Darshan Prajapati, Vineetha Ravindran, Jil Sutaria, and Pratik Patel. A comparative study of three phase 2-level vsi with 3-level and 5-level diode clamped multilevel inverter. *International Journal of Emerging Technology and Advanced Engineering*, 4(4):708–713, 2014.

[13] Riccardo Ruffo, Paolo Guglielmi, and Eric Armando. Inverter side rl filter precise design for motor overvoltage mitigation in sic-based drives. *IEEE Transactions on Industrial Electronics*, 67(2):863–873, 2019.

[14] Ouahid Bouakaz. *Contribution a l'analyse des onduleurs multi niveaux*. PhD thesis, Batna, Université El Hadj Lakhder. Faculté des Sciences de l'Ingenieur, 2005.

[15] Henni Abdelhadi Benblidia Med Karim. Modélisation d'un générateur pv par logique floue. 2021.

[16] Sorin Nadaban. From classical logic to fuzzy logic and quantum logic: a general view. *International Journal of Computers communications & control*, 16(1), 2021.

[17] Lotfi Asker Zadeh. Fuzzy sets. *Information and control*, 8(3):338–353, 1965.

[18] Azeddine Debbone and Mohamed Nadjib Meriem. Développement d'une commande dtc-svm de la machine asynchrone par logique floue. Master's thesis, Université Kasdi Merbah ouargla, 2023.

[19] Timothy J Ross. *Fuzzy logic with engineering applications*. John Wiley & Sons, 2005.

[20] Didier Dubois and Henri Prade. What are fuzzy rules and how to use them. *Fuzzy sets and systems*, 84(2):169–185, 1996.

[21] Soteris A Kalogirou. *Solar energy engineering: processes and systems*. Elsevier, 2023.

[22] Malika Fodil. *Commande adaptative par logique floue de la machine asynchrone*. PhD thesis, M'sila, Université Mohamed Boudiaf, 2008.

[23] Chuen-Chien Lee. Fuzzy logic in control systems: fuzzy logic controller. i. *IEEE Transactions on systems, man, and cybernetics*, 20(2):404–418, 1990.

[24] Mahesh Kumar Tiwari, Tithi Mall, and Akanksha Chaurasia. Review on pattern recognition with fuzzy logic.

[25] Yukun Cao and Yunfeng Li. An intelligent fuzzy-based recommendation system for consumer electronic products. *Expert Systems with Applications*, 33(1):230–240, 2007.

[26] Ching-Han Chen, Chien-Chun Wang, Yi Tun Wang, and Po Tung Wang. Fuzzy logic controller design for intelligent robots. *Mathematical Problems in Engineering*, 2017(1):8984713, 2017.

[27] Angela Torres and Juan J Nieto. Fuzzy logic in medicine and bioinformatics. *BioMed research international*, 2006(1):091908, 2006.